

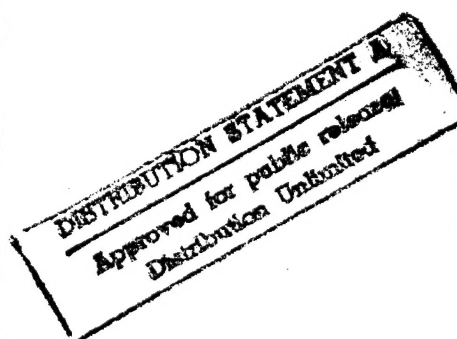
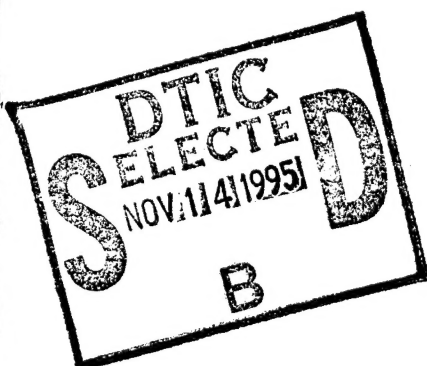
NB

CCM-80-15

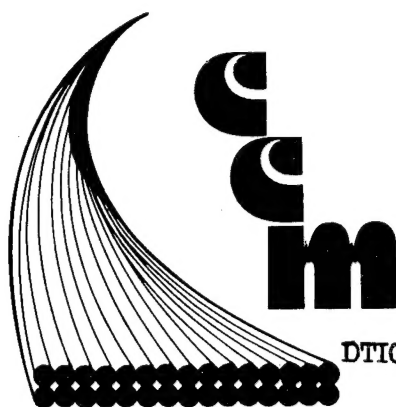
Center for Composite Materials

MATERIALS CHARACTERIZATION 1979-80:
TENSILE STRENGTH DATA VARIATION
AND NOTCH SENSITIVITY

ROBERT C. WETHERHOLD



19951019 160



DTIC QUALITY INSPECTED 5

College of Engineering
University of Delaware
Newark, Delaware

PLASTIC 39403

@*MSG DI4 DROLS PROCESSING - LAST INPUT IGNORED

*MSG DI4 DROLS PROCESSING-LAST INPUT IGNORED

-- 1 OF 1

DTIC DOES NOT HAVE THIS ITEM

-- 1 - AD NUMBER: D432696

-- 5 - CORPORATE AUTHOR: DELAWARE UNIV NEWARK CENTER FOR COMPOSITE
MATERIALS

-- 6 - UNCLASSIFIED TITLE: MATERIALS CHARACTERIZATION 1979-80: TENSILE
STRENGTH DATA VARIATION AND NOTCH SENSITIVITY,

--10 - PERSONAL AUTHOR: WETHERFOLD, R. C. ;

--11 - REPORT DATE: OCT , 1980

--12 - PAGINATION: 56P

--14 - REPORT NUMBER: CCM-80-15

--20 - REPORT CLASSIFICATION: UNCLASSIFIED

--22 - LIMITATIONS (ALPHA): APPROVED FOR PUBLIC RELEASE; DISTRIBUTION

-- UNLIMITED. ~~AVAILABILITY: CENTER FOR COMPOSITE MATERIALS, UNIVERSITY~~

-- ~~OF DELAWARE, 300 EVANS HALL, NEWARK, DE. 19711, CCM 80-15.~~

--33 - LIMITATION CODES: 1

-- END

Y FOR NEXT ACCESSION

END


Alt-Z FOR HELP3 ANSI

3 HDX 3

3 LOG CLOSED 3 PRINT OFF 3 PARITY

Materials Characterization 1979-80:

Tensile Strength Data Variation and
Notch Sensitivity



Robert C. Wetherhold

Center for Composite Materials
University of Delaware
Newark, Delaware 19711

October 1980

Abstract

A series of tensile strength tests were performed on a wide variety of sponsor supplied materials. A complete description of each material is given, and results are presented for unnotched and notched tensile strengths. The data are analyzed using Weibull, normal, and log normal statistics. The press-molded materials exhibit more scatter than the continuous or quasi-continuous processes. A system for estimating conservative design parameters is developed, and the results are applied to the unnotched tensile strength. Data are presented for tensile strength in the presence of a slit notch, and a method is given to calculate notched strength over a variety of notch sizes. Since the slit notch geometry gives the most strenuous stress concentration, the results may be used to give conservative estimates for other geometries. The use of "stress oriented" notched strength predictions is shown to be superior to that of classical Linear Elastic Fracture Mechanics (LEFM).

Accession For	
NTIS GRA&I	<input checked="" type="checkbox"/>
DTIC TAB	<input type="checkbox"/>
Unannounced	<input type="checkbox"/>
Justification <i>per printed label</i>	
By <i>DTIC AF memo 27 Nov 95</i>	
Distribution/	
Availability Codes	
Dist	Avail and/or Special
<i>A-1</i>	

Table of Contents

1. Material Descriptions and Test Geometry.	1
2. Summary of Test Results.	16
3. Data Analysis.	19
3.1 Inference of Weibull Parameters and Design Considerations.	19
Characterization of the Weibull Distribution	19
Statistical Inference of Weibull Parameters	21
Design Considerations of Weibull Statistics	25
3.2 Tensile versus Flexural Strength.	41
3.3 Inference of Normal and Log Normal Parameters and Design Considerations	43
Design Considerations of Normal Statistics	44
3.4 Notch Sensitivity	48
4. Discussion and Conclusions	59
Data and Statistics.	59
Data Variability	59
Notched Strength	61
Relationship between Notch Sensitivity and Tensile Data Variability	62

Introduction

The use of composite materials in load-bearing applications demands the use of reliability and statistical considerations. For metals design, this is covered by handbook "safety factors." Due to the variability of composite constituents and processing, suitable methods must be developed to calculate reliability. In addition, we must have assurance that the results are conservative so as to produce a reliable design. This report presents tensile strength data for a variety of composite material systems, and addresses the methods of analysis necessary for design.

Notches are important to consider in structural design, since they can be induced intentionally as cut-outs, or unintentionally as fabrication errors. There is a "notch size effect" in composites which demands improved methods of analysis over the classical "stress concentration factor" and "critical stress intensity factor" approaches. This report presents data for 3 notch sizes, and describes a method for predicting strength at other notch sizes.

1. Material Descriptions and Test Geometry

The following gives a description of the materials used in the 1979-80 Materials Characterization Program. The reinforcements include glass, graphite, and hybrid combinations; the molding processes include compression, injection, and pultrusion. Results are tabulated in section 2, and design and statistical considerations are discussed in section 3.

The materials were submitted in sheet form to the University of Delaware, and straight-sided tensile specimens were cut from sheet using a water-cooled surface grinder equipped with a diamond-impregnated cutting wheel. Bevelled end tabs of woven fiberglass were adhesively bonded to the specimen after the specimen surface was sanded. In addition, Material "F" was machined into a dogbone (see Figure 2) due to persistent failure in the grips. Material "D" was tested in flexure since no adequate adhesive could be found for this high tensile strength.

The asterisk (*) found on the material descriptions on the following pages denotes a registered trademark.

Material "A"

Supplied by ICI Americas

Material Description:

ITP-1054 Vinyl ester

25 w% XPL-1041 vinyl ester (half resin, half styrene)

50 w% OCF#433 glass (chopped), 1" length

25 w% camel-white CaCO_3

Compression molded at:

280°F

400 psi

2 minutes

charge 10" x 10" , final dimensions 12" x 12"

Specimen Geometry:

See figure 1; average thickness is 0.135".

Material "B"

Supplied by General Motors

Material Description:

SMC-R50 Vinyl ester

50 w% Dow Derakane 790 paste[†]

50 w% OCF 433AA-114 yield, 1" chopped glass

[†]paste consists of (parts by weight)

100 resin

1 T-butyl perbenzoate

100 camel white CaCO_3

2 Zinc stearate (mold release)

7 MgO slurry

Compression molded at:

300°F

600 psi

3 minutes

charge 18 3/4" x 12 1/2", final dimensions 21" x 24"

Specimen Geometry:

See figure 1; average thickness 0.142". Tensile direction is the 24" direction of the original panel.

Material "C"

Supplied by PPG Industries

Material Description:

XMC* - 3

weight percentages: Continuous glass 50.4 w%
PPG 1064-k15XMC strand

Chopped glass 21.6 w%
PPG 1064-k15XMC strand

Resin 28.0 w% PPG Selectron 50335
(semi-rigid)

molding conditions: 300°F, 500 psi, 3 minutes

charging and final dimensions: charge 8 1/8" x 16"
(centered), final dimensions 9" x 16" (continuous
glass in 16" direction).

Specimen Geometry:

See figure 1; average thickness is 0.109". Tensile
direction is in the continuous glass direction.

Material "D"

Supplied by General Electric

Material Description:

Pultruded glass/epoxy (No Commercial Designation)

79 w% glass, PPG 713 NT-16 Roving

21 w% Arnox* 3220 epoxy

Molding conditions:

die length 40"

die temperature 150°C

Resin bath temperature 60°C

Pultrusion rate 6"/min.

Post cure for 4 hours at 190°C

Specimen Geometry:

Straight-sided 1/2" wide x 3" long x 0.120" thick specimen for flexure data scatter test; 2" span for 3 point flexure. The length direction of the beam was in the pultrusion direction. No end tabs were used.

Material "E"

Supplied by International Harvester

Material Description:

SMC C45R20

35 w% Dow Derakane 790 vinyl ester

45 w% aligned, continuous glass OCF #433

20 w% random chopped glass OCF #433 (Length
Approximately 1")

ply sequence R/C, C/R, R/C, C/R where

R = random, C = continuous

Molding conditions:

300°F

1,000 psi

3 minutes

charge 11 1/2" x 17 1/2", final dimension 12" x 18"

continuous glass in 18" direction

Specimen Geometry:

See figure 1; average thickness 0.096". Tensile
direction is in the 18" direction of the original panel.

Material "F"

Supplied by E. I. Du Pont Co.

Material Description:

Rynite*545

45 w% chopped glass, 3/16" initial length

55 w% polyethylene terephthalate resin

molding conditions: Melt temperature 575°F(300°C)

Injection Pressure 8,000 psi

Mold fill time 1.2 sec

Mold temperature 100°C

Cycle time 46 sec

Dogbone specimens cut from 4" x 10" plaque per Figure 2.

Gating: Plaque was center end gated, with essentially
a point gate (very slight fan)

Specimen Geometry:

For tensile data scatter, see figure 2. For
notch sensitivity, see figure 1 except 10" total length.
Specimen thickness 0.125". Tensile direction was in the
mold-fill (10") direction.

Material "G"

Supplied by Graftek

Material Description:

Graftek molding compound Commercial Designation GT-50N

49 w% Zytel 101, Nylon 6-6

51 w% chopped graphite Manufacturer and

Length unknown

Molding conditions:

machine - Aurburg 221/221P 25 mm reciprocating screw

Unknown Injection Conditions

(temperature, pressure, mold-fill and cycle times)

Gating: end gated

Specimen Geometry:

See figure 3; average thickness 0.130". No notched strength tests were made due to insufficient width. Mold flashing was removed by a very light sanding.

Material "I"

Supplied by Ford Motor

Material Description:

R-65 Vinyl ester

67 w% OCF #411 roving, chopped 1" length

33 w% Dow Derakane 790 vinyl ester paste[†][†]paste composed of: (parts by weight)

100 Dow 790 resin

1 TBPB

20 snowflake CaCO_3

4 zinc stearate

2 Maglite D slurry

Molding conditions:

300°F

600 psi

3 minutes

Charge Size 12" x 24"; final dimensions 14" x 26"

Specimen Geometry:

See figure 1; average thickness 0.142". Tensile direction is the 26" direction of the original panels.

Material "J"

Supplied by Celanese

Material Description:

Graphite/Glass hybrid (No Commercial Designation)
 Unidirectional graphite faces, Celion 6000 fiber in
 PPG 50335 polyester resin, nominal 0.011" thick
 each face, Nominal 40 w% resin, 60 w% fiber
 HMC Core; 35 w% PPG 50335 polyester resin, 65 w%
 PPG type 518 Roving, 1" chopped; Semi Rigid
 (standard) Formula, Nominal 0.078" thick
 OVERALL ANALYSIS (EXPERIMENTALLY Determined):

$$\frac{\text{wt of faces}}{\text{total wt}} = 0.20$$

$$\frac{\text{wt of graphite fiber}}{\text{total wt}} = 0.12$$

MOLDING CONDITIONS:

305°F, 700 psi, for 3 min; "bumped" 3 times
 to release styrene to avoid surface bubbles
 charge approximate 80-85% for HMC core
 final dimensions 12" x 12"

Specimen Geometry:

See figure 1; average thickness 0.100". Tensile
 direction is in the 0° graphite fiber direction.

Material "L"

Supplied by Hercules

Material Description:

Graphite/Glass Hybrid (unknown commercial designation)

Unidirectional graphite, Hercules AS4P beamed fiber in

OCF E987 polyester resin

Core: C20R45, 65 w% OCF#433 AE113 Roving; (20 w%

continuous, 45 w%, 1" chopped glass) 35 w% OCF E987

polyester resin; C/R, R/C lay-up;

OVERALL ANALYSIS:

$$\frac{\text{wt glass fiber}}{\text{total wt}} = 0.501$$

$$\frac{\text{wt carbon fiber}}{\text{total wt}} = 0.133$$

$$\frac{\text{wt resin}}{\text{total wt}} = 0.365$$

$$\frac{\text{wt carbon fiber}}{\text{wt graphite skin layers}} = 0.383$$

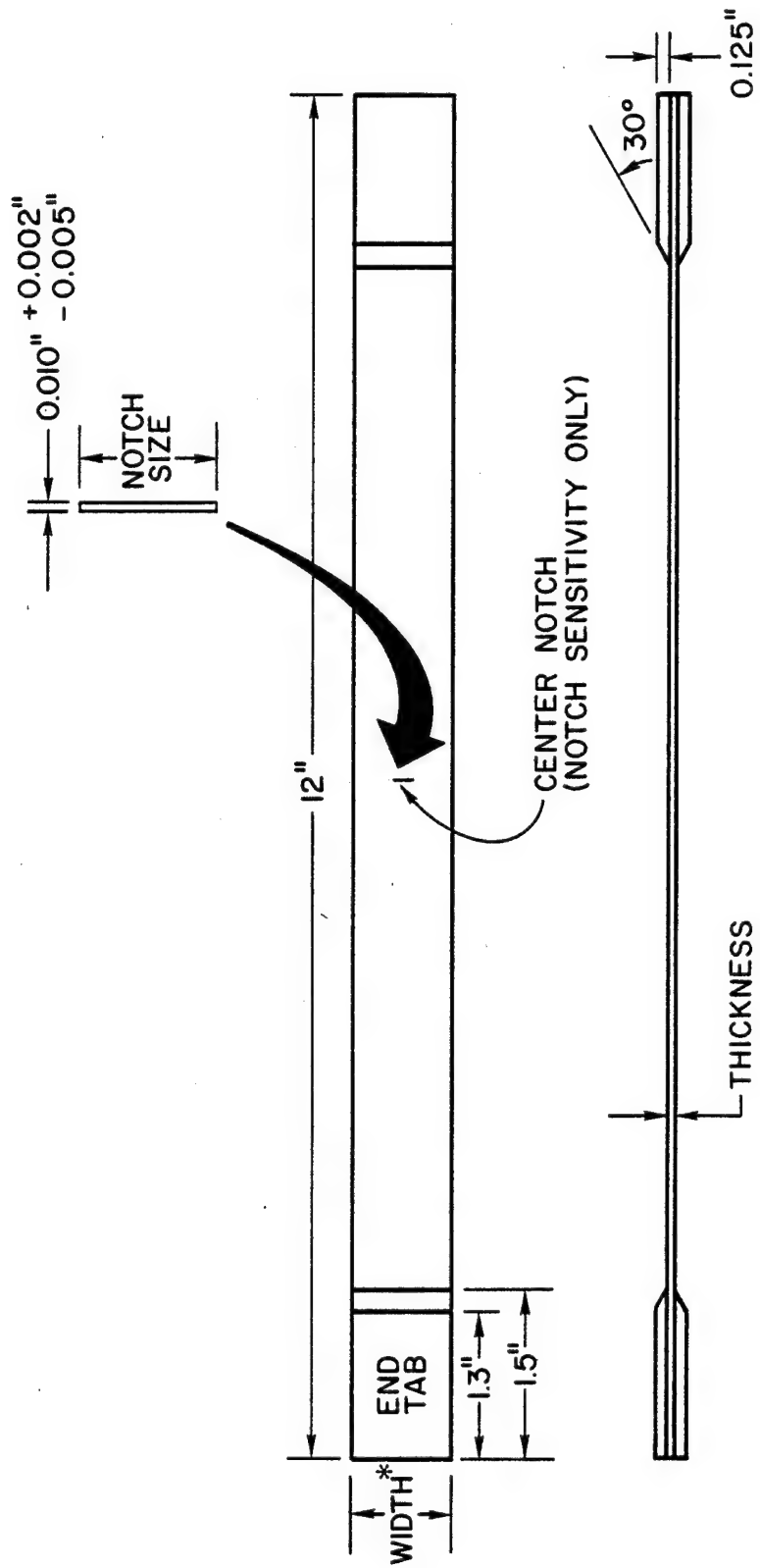
Processing:

SMC made to nominal 65 % fiber loading with slightly resin-rich carbon fiber plies (due to difference in wet-out characteristics) on conventional SMC - C/R machine. Molded in 12" by 18" matched metal mold 3 min. at 1000 psi and 300°F. Continuous carbon fiber skins were placed over a balanced,

symmetric core of C20R45 (20 wt% continuous, 45 wt% 1" random chopped glass) glass core with all continuous reinforcement aligned in a parallel fashion (the innermost reinforcement is chopped glass).

Specimen Geometry:

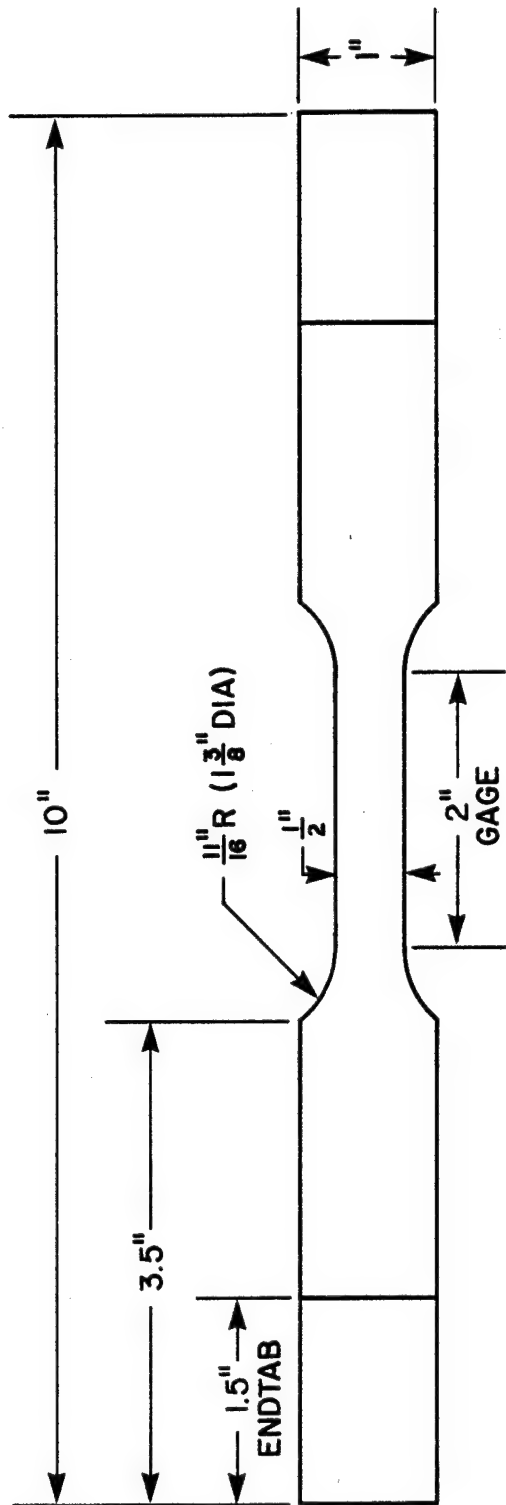
See figure 1; average thickness 0.101". Tensile direction is the continuous fiber direction.



*1.0" FOR DATA SCATTER
1.5" FOR NOTCH SENSITIVITY

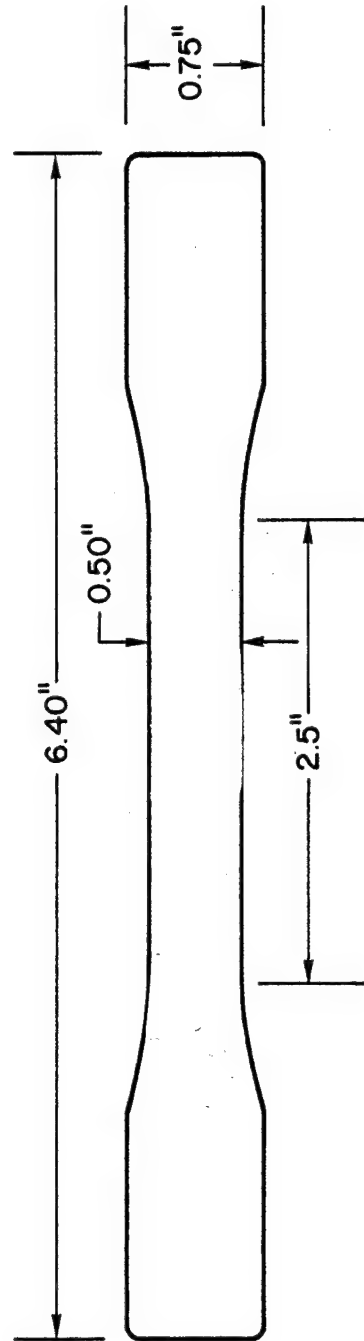
TENSILE SPECIMEN GEOMETRY

Figure 1.



MATERIAL "F" TENSILE SPECIMEN
SCALE: 3/4 SIZE

Figure 2.



**TENSILE SPECIMEN
MATERIAL "G"**

(END TABS OMITTED FOR CLARITY)
PER ASTM D-647

Figure 3.

2. Summary of Test Results

The tensile strength results are shown in Table 1. The strengths have been analyzed by fitting the data to three statistical models: Weibull, Normal, and Log-Normal. The meaning of the inferred statistical results is explained in Section III (Data Analysis). All specimens were tested in tension, 25 replicates, except material "D," which was tested in flexure.

The notched strength results are presented in Table 2. The specimens have an ultrasonically machined, very thin, center notch. Each notch size for each material has 5 replicates. Specimens of material "G" were too narrow to permit notched strength tests. Material D showed extensive axial splitting and end tab debonding, due to its high ultimate strength.

Table 1
Tensile Data Scatter

Material	Material Type ¹	Weibull Statistics		Normal Statistics		Log ₁₀ Normal Statistics	
		Shape Parameter α	Location Parameter β (psi)	Average \bar{X} (psi)	Standard Deviation S (psi)	X_{LOG} ($\sqrt{\text{psi}}$)	S_{LOG} ($\sqrt{\text{psi}}$)
A	SMC-R	16.6	23,200	22,480	1720.	4.35	0.0346
B	SMC-R	12.9	26,400	25,400	2080.	4.41	0.0354
C	XMC*	21.6	85,500	83,600	4222.	4.92	0.0220
D	Pultruded	41.1	167,000 ²	164,800 ²	4781.	5.21	0.0127
E	SMC-C/R	27.6	113,000	111,500	4101.	5.05	0.0160
F	Inj. Molded	17.9	19,800 ³	19,310 ³	968.2	4.29	0.0215
G	Inj. Molded (graphite)	95.2 ⁴	31,800 ⁴	31,600	394.8	4.50	0.00545
I	SMC-R	35.9	32,700	32,280	948.8	4.51	0.0128
J	Hybrid glass/graphite	14.8	57,300	55,600	3920	4.74	0.0307
L	Hybrid glass/graphite	10.9	75,800	72,850	7266.	4.86	0.0446

¹ Glass reinforcement unless otherwise noted.

² Results for flexure (see section 3.2).

³ Value for specimens machined from 4" x 10" flat plaque. As-molded ASTM dogbones yield 28,000 psi tensile strength.

⁴ Results for flexure (see section 3.2).

Table 2
Notched Tensile Strength

Material	Crack-length (in) 2c	Nominal Strength σ_N psi	"True" Strength ¹ σ_N^∞ psi	Critical Stress Intensity Factor ² k_{Ic} psi $\sqrt{\text{in}}$
A	0.126	21,800	21,900	9,730
	0.250	16,700	16,900	10,600
	0.375	14,900	15,300	11,700
B	0.125	24,100	24,200	10,700
	0.253	19,600	19,800	12,500
	0.375	16,800	17,500	13,400
C	0.127	65,600	65,800	29,400
	0.250	52,500	53,100	33,300
	0.375	48,900	50,200	38,500
E	0.125	97,500	97,800	43,300
	0.250	87,600	88,600	55,500
	0.375	75,600	77,600	59,900
F	0.125	13,100	13,200	5,820
	0.250	10,400	10,500	6,590
	0.375	8,530	8,760	6,720
I	0.125	26,300	26,400	11,700
	0.256	22,300	22,600	14,300
	0.375	18,800	19,300	14,800
J	0.125	56,500	56,700	25,100
	0.250	45,600	46,100	28,900
	0.375	38,800	39,800	30,600
L	0.125	68,200	68,400	30,300
	0.250	53,000	53,600	33,600
	0.375	49,000	50,300	38,600

1. $\sigma_N^\infty = (\text{FWC}) \sigma_N$

σ_N = avg. measured failure stress

FWC = Finite Width Correction factor

$$= \left[\frac{W}{\pi c} \tan \left(\frac{\pi c}{W} \right) \right]^{1/2} \quad [\text{Paris \& Sih}]$$

where W = width at specimen = 1.50 in.

c = crack half-length

the $\left(\frac{\pi c}{W} \right)$ argument is in radians

2. $k_{Ic} = \text{critical stress intensity factor} = \sigma_N^\infty \sqrt{\pi c}$

3. DATA ANALYSIS

3.1 Inference of Weibull Parameters and Design Considerations

• Characteristics of the Weibull Distribution

The generally used form for a cumulative distribution function (or simply "distribution function")

F is:

$$F(\sigma) = P(\sigma_s \leq \sigma) \quad (1)$$

where σ_s is a random variable*, P denotes probability, and σ is the particular value of interest. For a set of data which obeys a Weibull distribution, the distribution function is:

$$F(\sigma) = 1 - \exp[-(\sigma/\beta)^\alpha] \quad \sigma \geq 0 \quad (2)$$

where exp is exponential function

β is the scale or location parameter

α is the shape parameter

Mathematicians often use the equivalent notation

$$\sigma \overset{d}{\sim} W(\beta, \alpha) \quad (3)$$

to show that σ obeys a Weibull distribution. If σ_s is the tensile strength and σ is the applied stress, then $F(\sigma)$ represents the probability of failure.

We are often interested in the reliability, i.e. the probability that the random variable (outcome of an experiment) exceeds the particular value of interest.

* A "random variable" is simply the outcome of an experiment. For example, the value shown on a fair die after a die toss is a random variable.

This reliability is expressed as

$$R(\sigma) = P(\sigma_s \geq \sigma) \quad (4)$$

or

$$R(\sigma) = 1 - F(\sigma)$$

and, for a Weibull distribution, is given by:

$$R(\sigma) = \exp[-(\sigma/\beta)^\alpha] \quad \sigma \geq 0 \quad (5)$$

If σ_s is the tensile strength and σ is the applied stress, then $R(\sigma)$ represents the probability of survival.

The mean or average of the population can be expressed in terms of α, β as

$$\bar{\sigma} = \beta \Gamma(1 + 1/\alpha) \quad (6)$$

where Γ is the Gamma function, a table look-up. For $\alpha \geq 1$, which is the normal case for strength results, $0.886 \leq \Gamma \leq 1$, so that $\bar{\sigma} \leq \beta$. The average is slightly less than the scale parameter due to the skewness of the distribution. The standard deviation for a Weibull distribution is:

$$\text{Std. Dev. } S = \beta [\Gamma(L + 2/\alpha) - \Gamma^2(1 + 1/\alpha)]^{1/2} \quad (7)$$

• Statistical Inference of Weibull Parameters

Given a set of sample data from an experiment, we would like to predict estimates α and β for the entire (infinite) population. One way to do this is by solution of the maximum likelihood equations; this requires use of a computer or programmable calculator. The second method is by the use of logarithms; this method should be used only if a digital computer or programmable calculator is not available.

Maximum Likelihood Method

This method has a sound theoretical basis and allows interval estimates to be made for the statistics α, β . It demands solution of a very non-linear equation, but is routine with a computer or programmable calculator.

The maximum likelihood estimator $\hat{\theta}_n$ for a set of n random variables X_i is given by the solution of:

Define Likelihood

$$L(\theta) = f(x_1; \theta) f(x_2; \theta) \dots f(x_n; \theta) \quad (8)$$

and for Weibull Distribution,

$$\text{MAX } L(\theta) = \prod_{i=1}^n \frac{\alpha}{\beta} \left(\frac{x_i}{\beta} \right)^{\alpha-1} \exp \left[- \left(\frac{x_i}{\beta} \right)^{\alpha} \right] \quad (9)$$

where f is the p.d.f. of X , and θ is the true population parameter, and $L(\theta)$ reaches a maximum at $\hat{\theta}$ [Mann, Schafer,

and Singpurwalla]. The maximization equation (9) acts to maximize the likelihood of "legitimizing" the outcome of a given experiment [Mendenhall and Schaeffer].

The maximum likelihood equations for $\hat{\alpha}, \hat{\beta}$ are given by:

$$k(\hat{\alpha}) = 0 = \frac{\sum_{i=1}^n x_i^{\hat{\alpha}} \ln x_i}{\sum_{i=1}^n x_i^{\hat{\alpha}}} - \frac{1}{\hat{\alpha}} - \frac{\sum_{i=1}^n \ln x_i}{n} \quad (10)$$

$$\hat{\beta} = \left(\frac{1}{n} \sum_{i=1}^n x_i^{\hat{\alpha}} \right)^{1/\hat{\alpha}} \quad (11)$$

The $\hat{\alpha}, \hat{\beta}$ are point estimates to the true population parameters α, β [Mann, et al.]. In practice, equation (10) is solved for $\hat{\alpha}$ and the result used in (11) to get $\hat{\beta}$. For small sample sizes ($n < 30$), the estimates $\hat{\alpha}, \hat{\beta}$ from equations (10, (11) are biased. Fortunately, there are correction factors available which depend only on n , the number of data points [Thoman, Bain, and Antle]. These correction factors $B(n)$, shown below, thus provide unbiasing so that

$$E[B(n)\hat{\alpha}] = \alpha \quad (12)$$

Table 3

Unbiasing Factors B(n) for MLE of α

n	5	6	7	8	9	10	11	12	13	14	15	16
B(n)	.669	.752	.792	.820	.842	.859	.872	.883	.893	.901	.908	.914
n	18	20	22	24	26	28	30	32	34	36	38	40
B(n)	.923	.931	.938	.943	.947	.951	.955	.958	.960	.962	.964	.966
n	42	44	46	48	50	52	54	56	58	60	62	64
B(n)	.968	.970	.971	.972	.973	.974	.975	.976	.977	.978	.979	.980
n	66	68	70	72	74	76	78	80	85	90	100	120
B(n)	.980	.981	.981	.982	.982	.983	.983	.984	.985	.986	.987	.990

One thus solves equation (10) for $\hat{\alpha}$, unbias the estimate by multiplying it by B(n) from Table 3, and then solves for $\hat{\beta}$.

Logarithm Method

The data are ranked from lowest to highest, and a ranking statistic is used. The rank can be simple, mean, median, hazard, or Hazen; but there is a preference for the median rank.* This median rank is applied to the ranked data as

P_j from tables

or

$$P_j \approx \frac{j - 0.3}{n + 0.4} \quad (13)$$

* Simple Rank $P_j = j/n$

Mean Rank $P_j = j/n+1$

Hazen Rank $P_j = \frac{j-0.5}{n}$

which gives a series of j ranks of the n total data points. This rank statistic is used as an approximation to the distribution function F . It is helpful to draw a graph of data value (abscissa) versus rank (ordinate).

We proceed to manipulate the formula (2) into a convenient linear form. Since $P(\sigma_s \leq \sigma) = F(\sigma)$,

$$1 - F = \exp[-(\sigma/\beta)^\alpha] \quad (14)$$

Taking natural logarithms,

$$\ln(1 - F) = -(\sigma/\beta)^\alpha \quad (15)$$

Clearing the minus sign and again taking natural logarithms,

$$\ln(-\ln(1 - F)) = \alpha \ln(\sigma/\beta) \quad (16a)$$

or

$$\ln \sigma = \frac{1}{\alpha} \ln[-\ln(1 - F)] + \ln \beta \quad (16b)$$

The equation (16b) is in linear form for a least squares analysis of data points $\ln \sigma$ versus $\ln[-\ln(1 - \text{Rank})]$. The slope is $1/\alpha$, and $\ln \beta$ can be easily calculated. "Weibull function" probability paper exists which has the transformation (16b) implicit in its scale.

Note that the form (16b) is also usable to calculate an allowable σ for a given structural reliability $R = 1 - F$, once the α and β are known.

Problems with logarithm method: The α, β found by linear regression on (16b) are "point estimates." To obtain meaningful interval estimates of say α requires us to assume that the least squares statistics $1/\alpha$ and $\ln \hat{\sigma}$ are normally distributed. This assumption seems doubtful at best. The logarithm method also has difficulty handling censored data points, which can occur in fatigue experiments (as run-out, etc.).

• Design Considerations of Weibull Statistics

The estimates $\hat{\alpha}, \hat{\beta}$ of the population parameters α, β shown in Table 1 are derived by using data and solving Maximum Likelihood equations. These estimates, then, are themselves distributed; re-running the experiment could produce different estimates. We would like to choose our estimates so that we conservatively underestimate the reliability. This can be seen from figure 4. Any time we predict a reliability that is lower than the actual reliability as determined by experiment using a ranking formula, we are conservative.

We would like to use our estimates for α and β , and "downgrade" them in a systematic manner so as to minimize our predicted reliability. Since a designer would never use a failure stress greater than the average, consider the region $X \leq \bar{X} \leq \beta$.

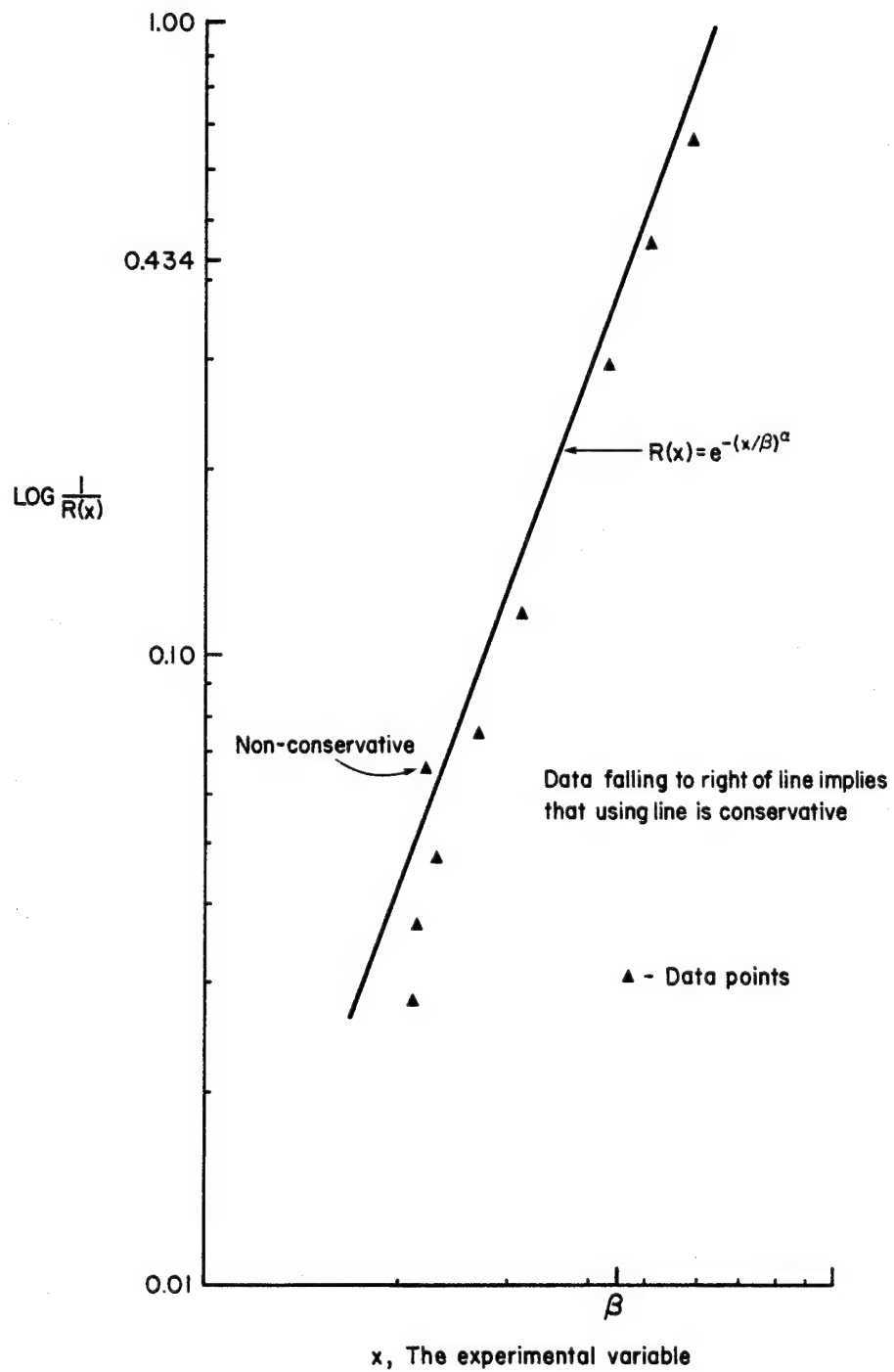


Figure 4.

If we choose lower bounds $\alpha_L < \hat{\alpha}$, $\beta_L < \hat{\beta}$, we minimize the predicted reliability for any stress less than the mean. This can be expressed as

$$R(x; \alpha_L, \beta_L) = e^{-(x/\beta_L)^{\alpha_L}} < e^{-(x/\beta)^{\alpha}} = R(X; \alpha, \beta) \quad (17)$$

$$\begin{aligned} \text{for } \alpha_L &< \alpha \\ \beta_L &< \beta \\ x &< \beta \end{aligned}$$

See figure 5.

Using information from [Thoman, et al.], we get the following relations to get one-sided 95% confidence limits for α and β :

$$\begin{aligned} \alpha_L &= \hat{\alpha}/l_\gamma & l_\gamma &= 1.381 \text{ for } n = 25 \\ \beta_L &= \hat{\beta} \exp\left(-\frac{l_\gamma}{2}\right) & l_\gamma &= 0.3705 \text{ for } n = 25 \end{aligned} \quad (18)$$

The only conceptual difficulty in using the results of [Thoman et al.] is that the lower estimates α_L , β_L are found by searching out upper estimates for the functions $\hat{\alpha}/\alpha$ and $\hat{\alpha} \ln(\hat{\beta}/\beta)$. The convenient aspect of the use of "percentage points" l_γ is that it is independent of the particular values of the estimates $\hat{\alpha}, \hat{\beta}$.

The values for α_L , β_L are shown in Table 4. The plots of tensile strength data, and curves for the

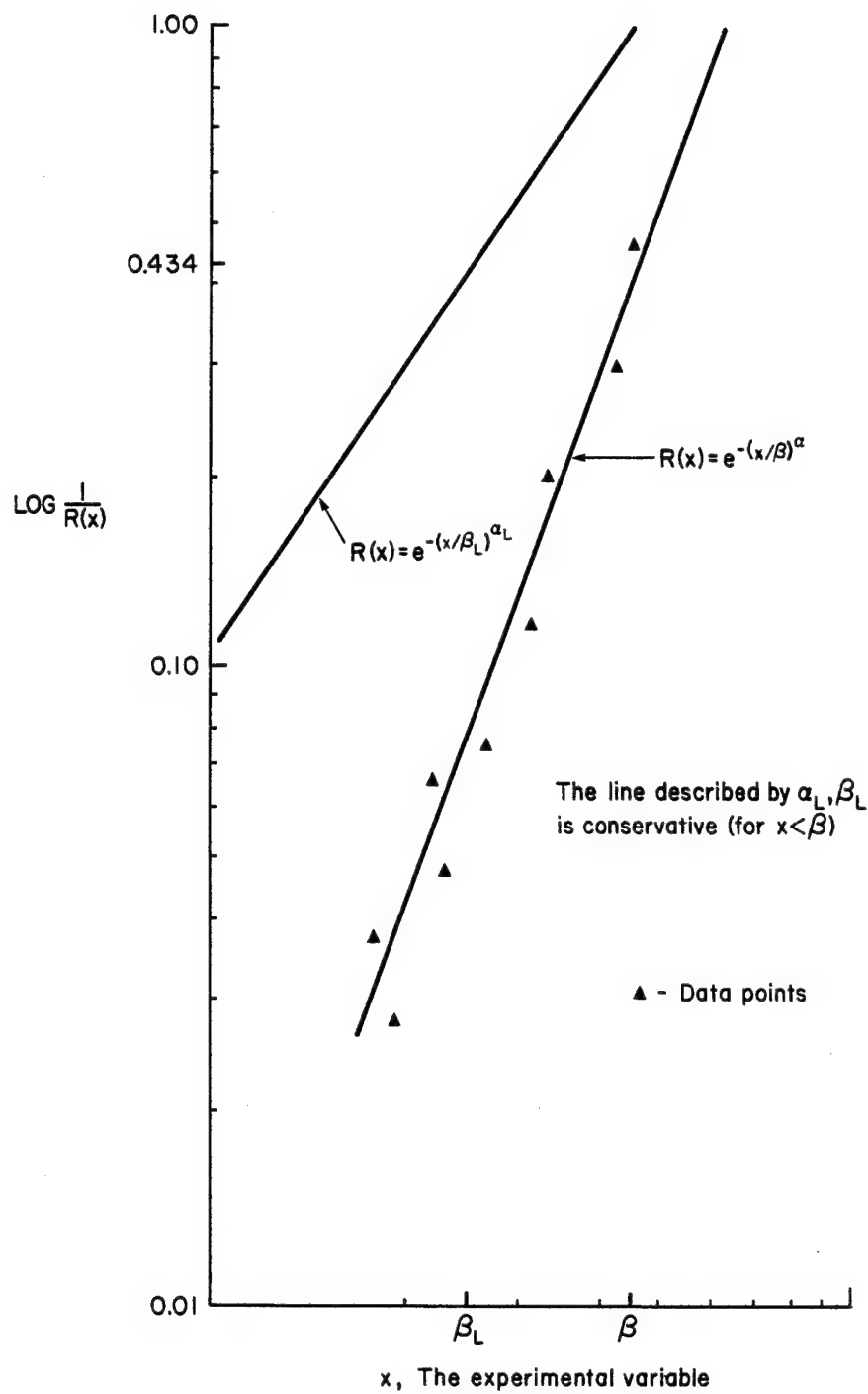


Figure 5.

estimates $\hat{\alpha}, \hat{\beta}$ and the lower bound estimates α_L, β_L are shown in figures 6 through 15. The curves using α_L, β_L are uniformly conservative, as all data points fall below them. We thus predict a lower reliability than we actually see.

Table 4
Lower Bound (Conservative) Values
for Weibull Parameters

Material	MLE point estimates		Lower Limits for 95% Confidence	
	$\hat{\alpha}$	$\hat{\beta}$ (psi)	α_L	β_L (psi)
A	16.6	23,200	12.0	22,700
B	12.9	26,400	9.34	25,600
C	21.6	85,500	15.6	84,000
D	41.1	167,000	29.8	166,000
E	27.6	113,000	20.0	111,000
F	17.9	19,800	13.0	19,400
G	95.2	31,800	68.9	31,700
I	35.9	32,700	26.0	32,400
J	14.8	57,300	10.7	55,800
K	10.9	75,800	7.89	73,200

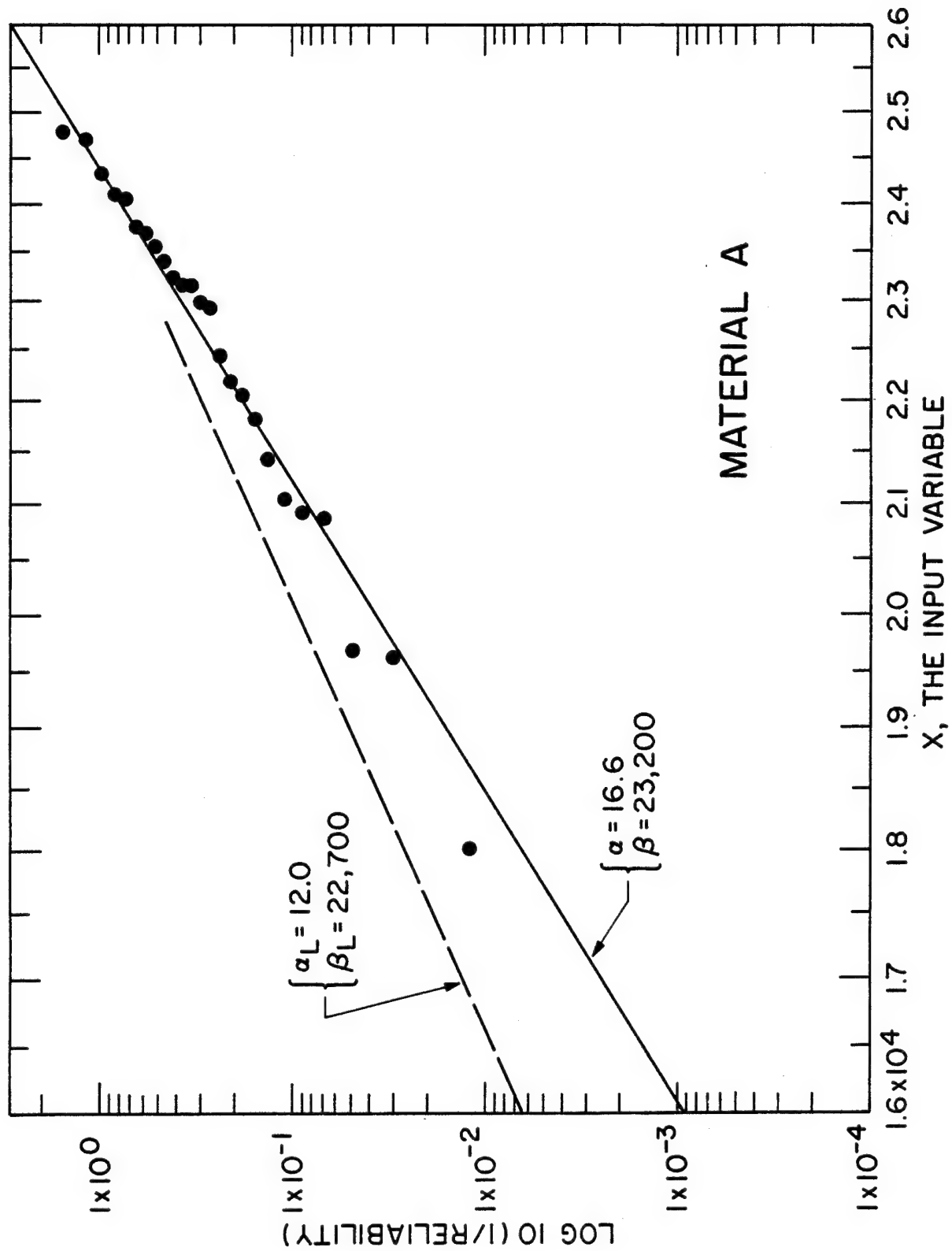


Figure 6.

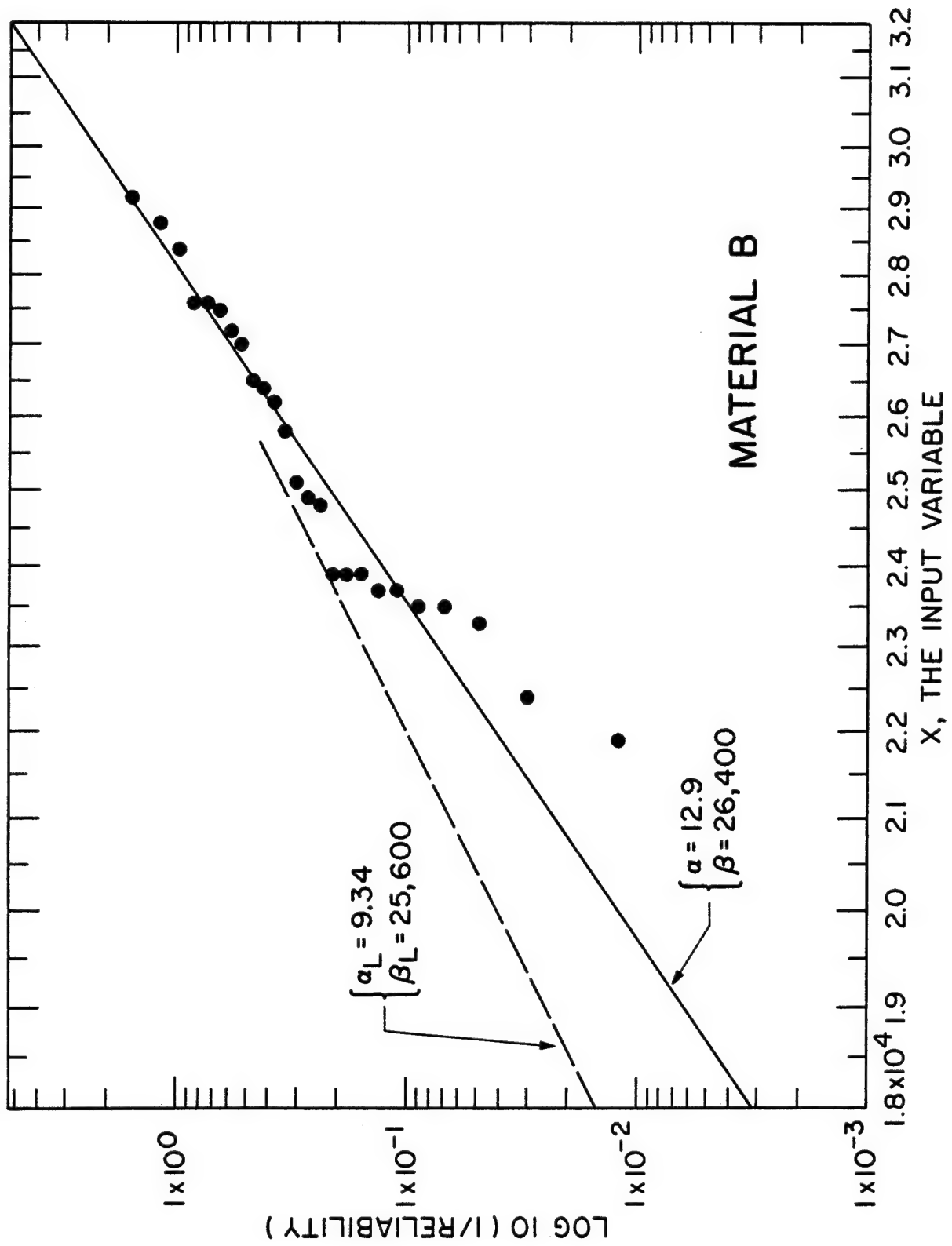


Figure 7.

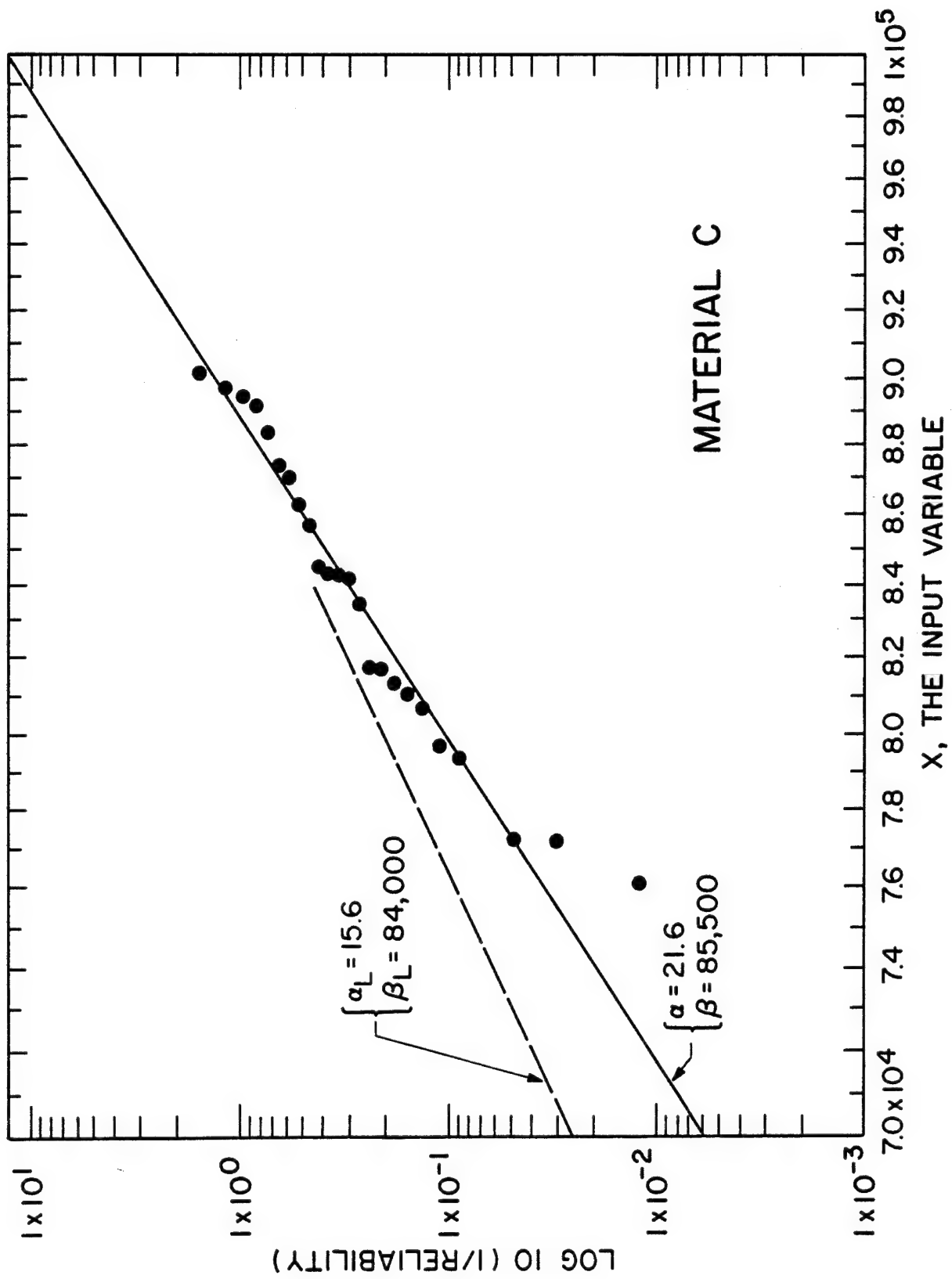


Figure 8.

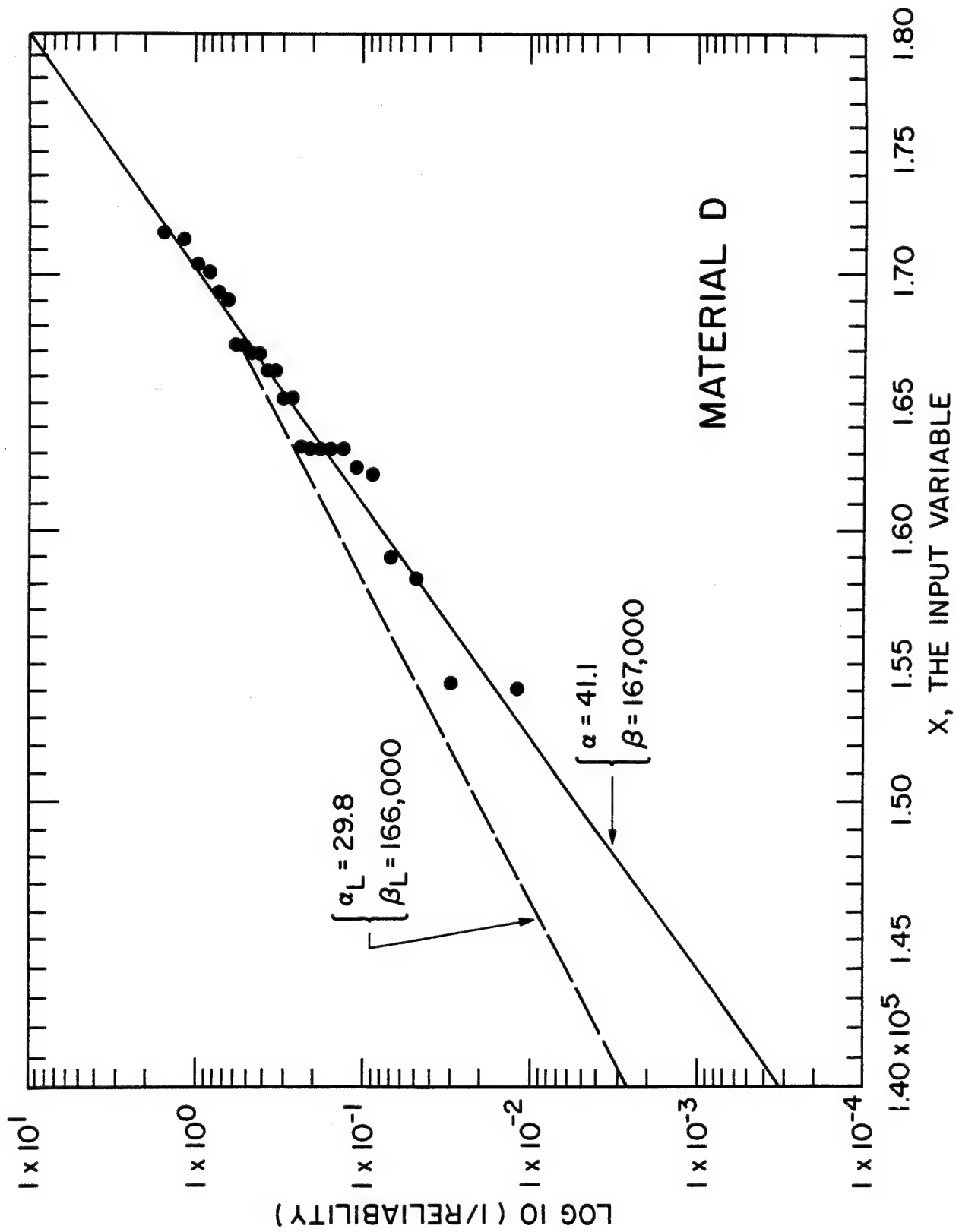


Figure 9.

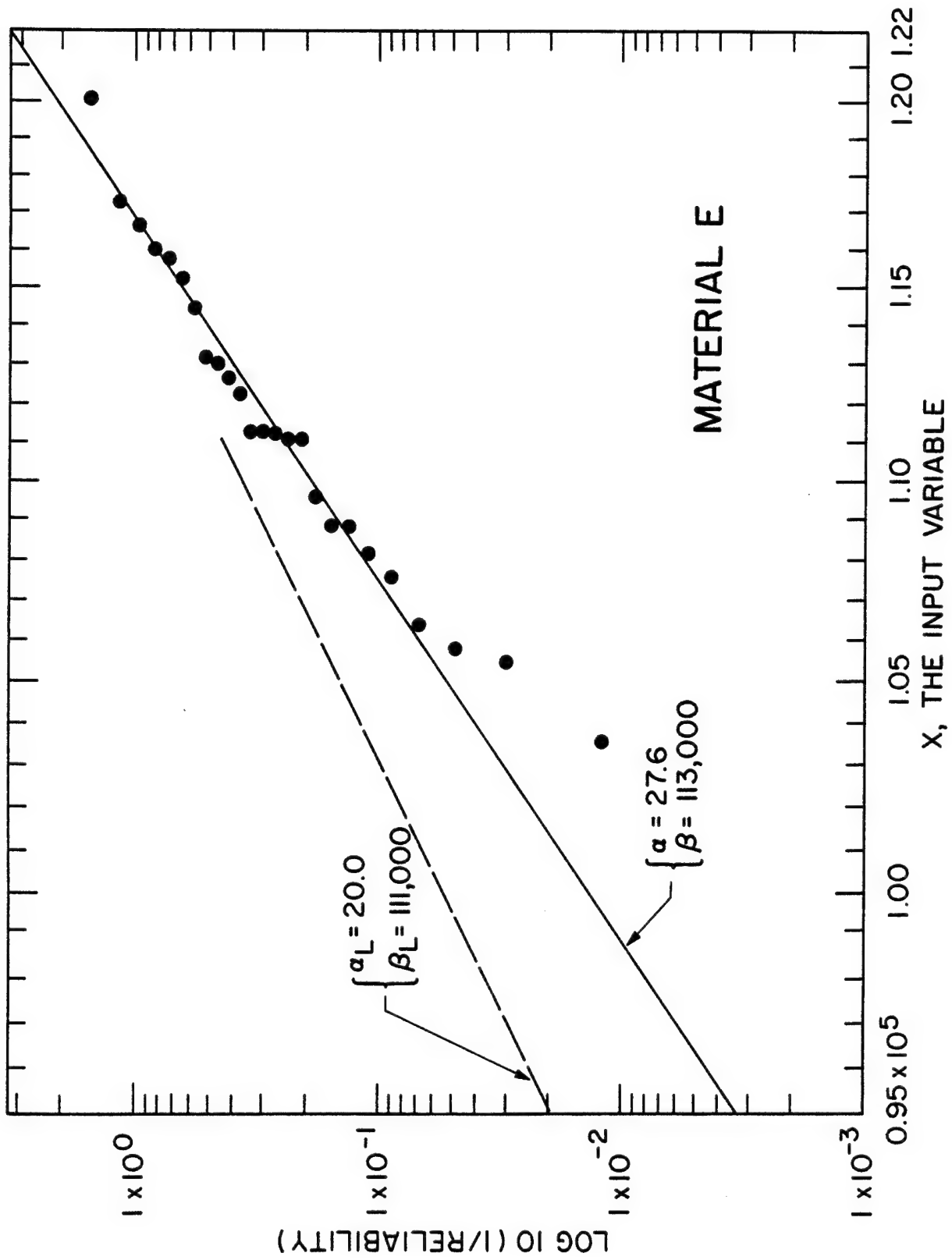


Figure 10.

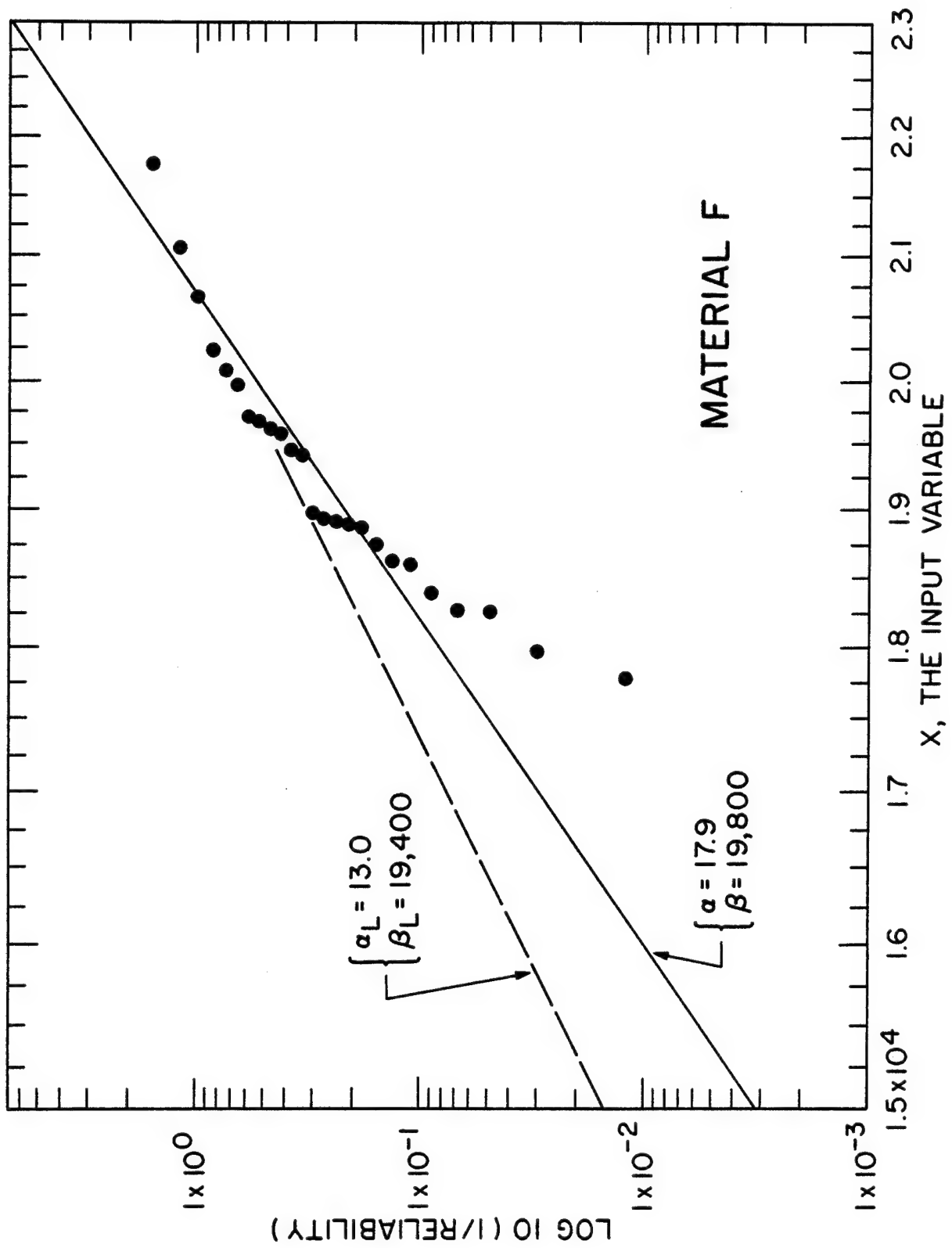


Figure 11.

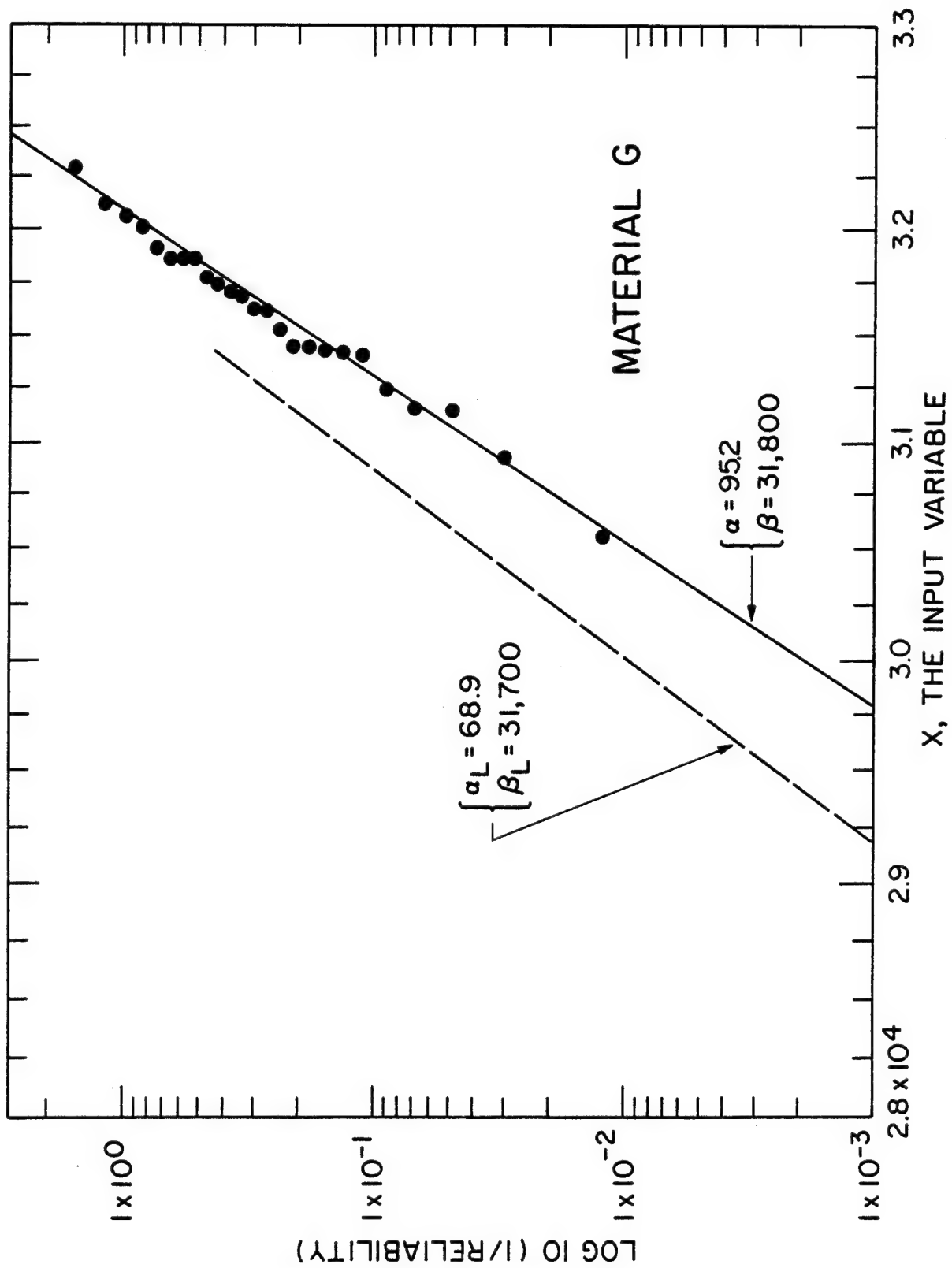


Figure 12.

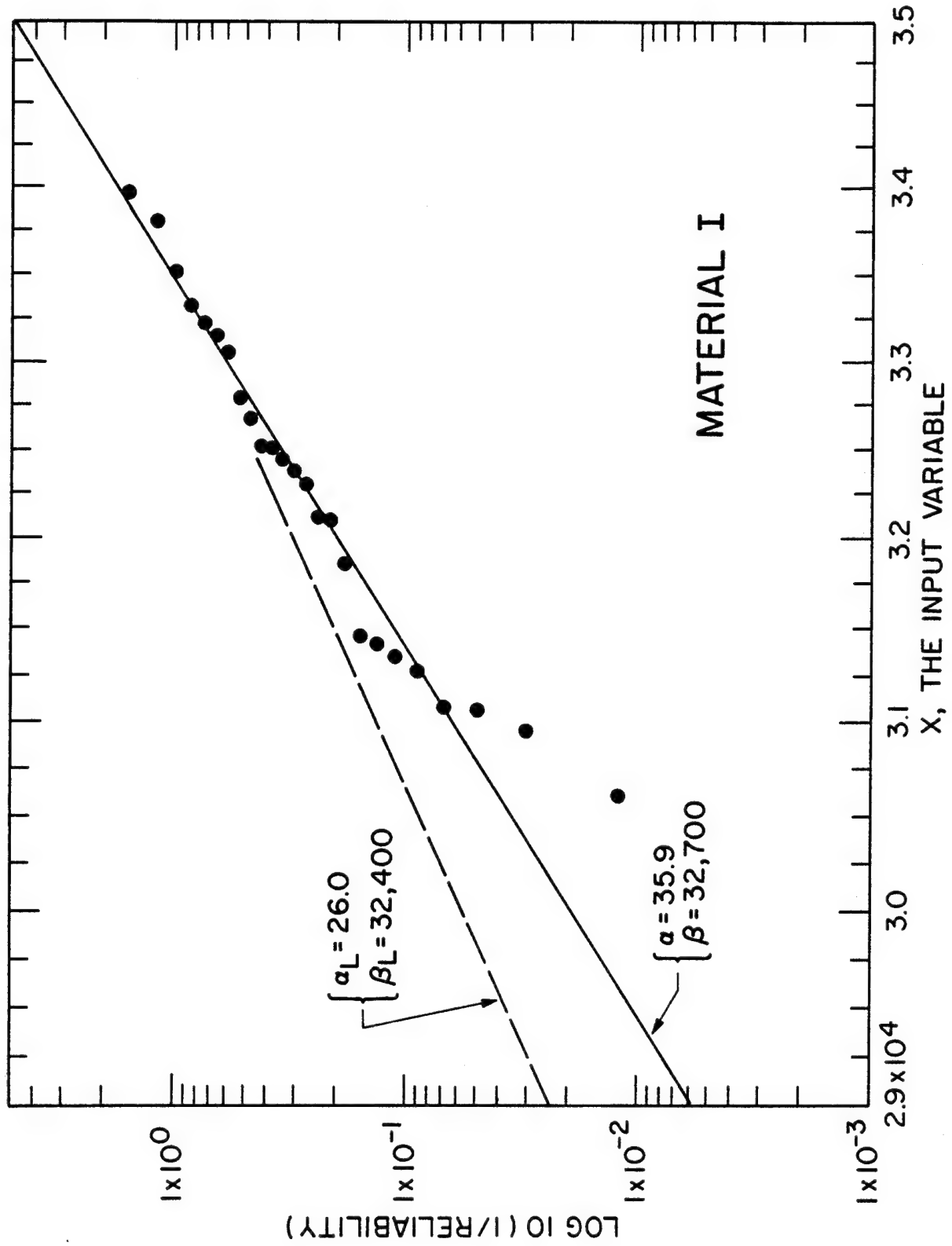


Figure 13.

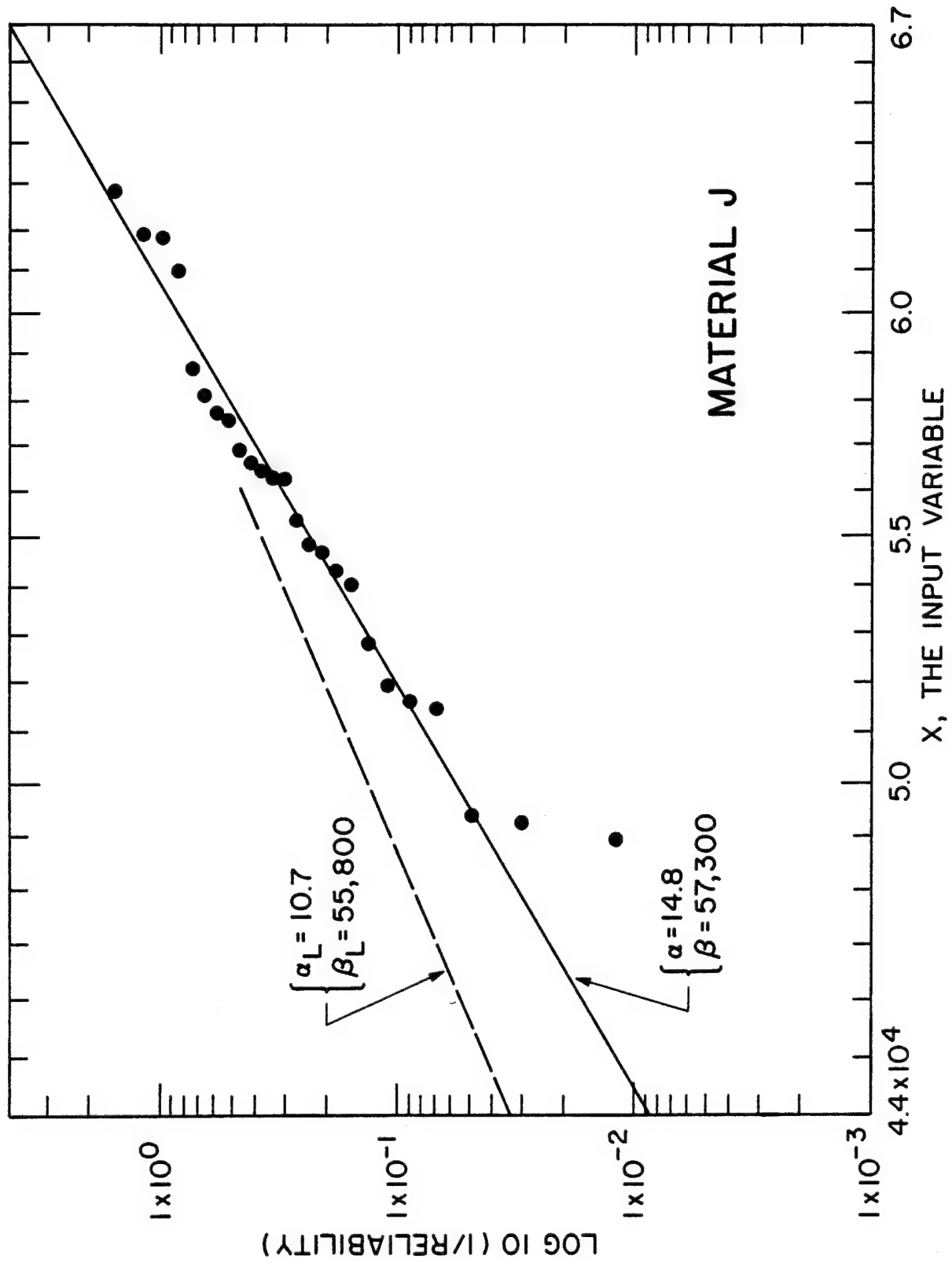


Figure 14.

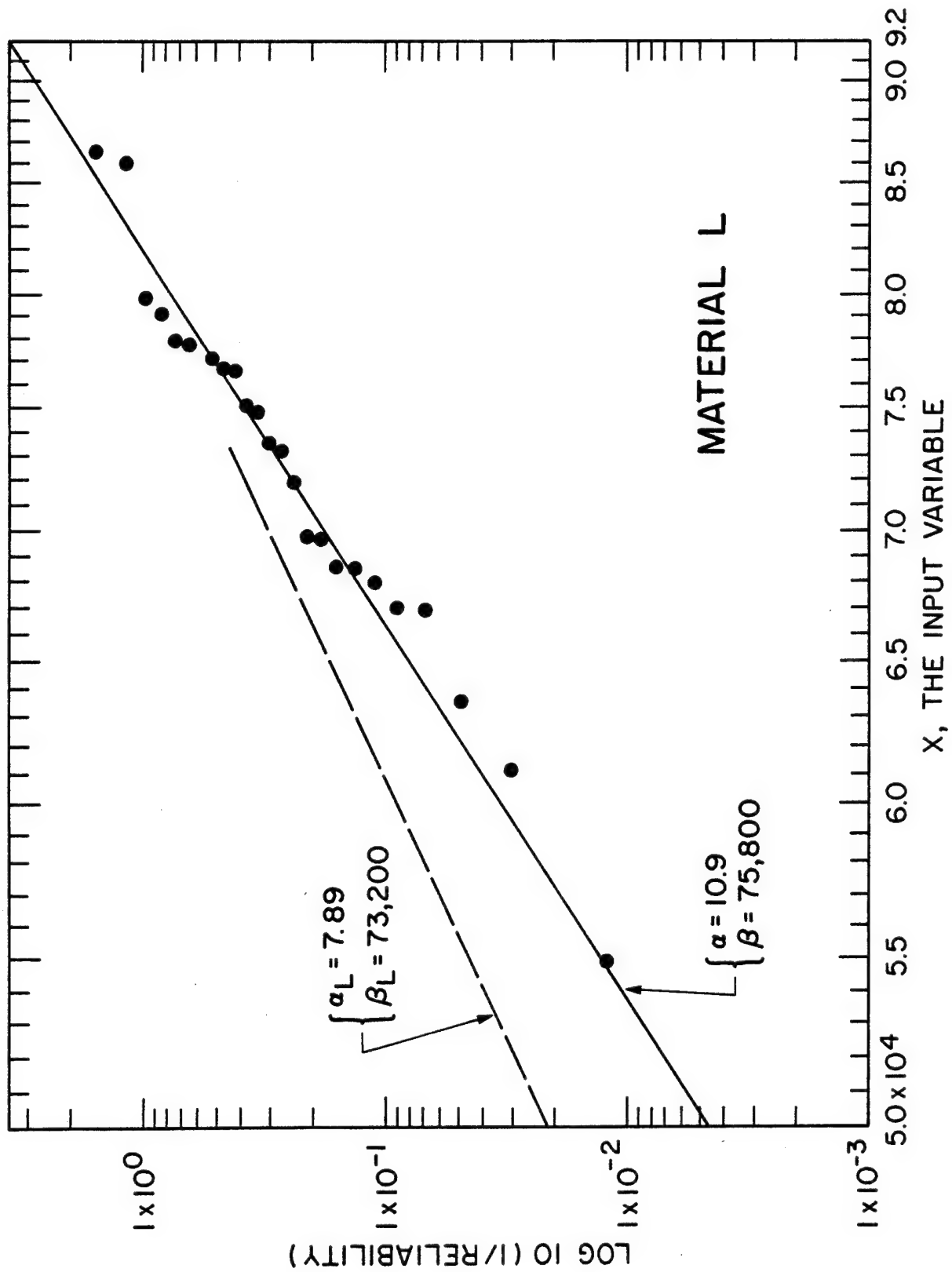


Figure 15.

3.2 Tensile vs. Flexural Strength

For a homogeneous brittle material, the flexural strength is often higher than the tensile strength. This has been explained by [Bullock] as a volume effect of the stresses. The reasoning uses the Weibull formulation for reliability of a material under tensile stress:

$$R(\sigma) = \exp \left\{ - \int_V (\sigma/\beta_0)^\alpha \right\} \quad (19)$$

where V is the volume under tension

When the integral (19) is evaluated for a tensile volume, it gives:

$$R(\sigma) = \exp \left[-(\sigma/\beta_T)^\alpha \right] \quad (20)$$

where $\beta_T = \beta_0 (V_T)^{-1/\alpha}$

and V_T = tensile volume

When the integral (19) is evaluated for a 3 point flexural specimen, it gives:

$$R(\sigma) = \exp [-(\sigma/\beta_F)^\alpha] \quad (21)$$

where $\beta_F = \beta_0 \left[\frac{2(\alpha + 1)}{V_f} \right]^{1/\alpha}$

and V_f is the total volume of the flexural specimen
(assume equal tensile and compressive modulus)

The same volume of material V , if tested in tension and 3-point flexure, gives a ratio of average strengths as follows:

$$\frac{\bar{\sigma}_T}{\bar{\sigma}_F} = \frac{\beta_T \Gamma(1 + 1/\alpha)}{\beta_F \Gamma(1 + 1/\alpha)} \quad (22a)$$

or

$$\frac{\bar{\sigma}_T}{\bar{\sigma}_F} = \frac{1}{[2(\alpha + 1)]^{1/\alpha}} \quad (22b)$$

For material "D," tested in flexure, the predicted average tensile strength would be

$$\begin{aligned} \bar{\sigma}_T &= 167,000 \text{ psi } [0.898] \\ &= 150,000 \text{ psi} \end{aligned}$$

Note also that the volume effect predicted from (20) or (21) is relatively mild. Doubling the volume with shape parameter $\alpha = 20$ only decreases the average strength by a factor of 1.035, for example. A cautionary note should be added that some experimental results have been found which contradict the simple relation (22) [Whitney and Knight].

3.3 Inference of Normal and Log Normal Parameters and Design Considerations

The tensile strength data may also be analyzed by fitting it to a normal distribution. The standard normal statistics are used to give the results found in Table 1, mainly:

$$\text{Average } \bar{X} = \sum_i X_i / n \quad (23)$$

$$\text{Std. Deviation } S = \sqrt{\frac{\sum (X_i - \bar{X})^2}{n-1}} \quad (24a)$$

$$= \sqrt{\frac{\sum X_i^2}{n-1} - \frac{n}{n-1} \bar{X}^2} \quad (24b)$$

The log normal statistics shown in Table 1 are the result of assuming that the log of the strength may be normally distributed. Thus we define a new variable

$$Y = \log_{10} X \quad (25)$$

and operate on Y by using equations (23) and (24). This yields a mean \bar{X}_{LOG} and standard deviation S_{LOG} as shown in the summary, Table 1.

Design Considerations of Normal Statistics

We would like to obtain extreme bound estimates so that we minimize the predicted reliability. That is, we need to predict a probability of failure based on our estimate which always exceeds the experimental probability of failure determined by ranking. (See section 3.1). The probability of failure is

$$P[\sigma_s \leq a] = \Phi(z) \quad (26)$$

where σ_s is random variable of strength

a is particular specified stress

Φ is the normal function,

$$\Phi(z) = \frac{1}{\sqrt{2\pi}} \int_{-\infty}^z e^{-y^2/2} dy$$

z is the "standard" (reduced) variable, $\frac{a-\bar{X}}{s}$
 s is the standard deviation
 \bar{X} is the average strength

Since Φ increases with increasing z , we choose bounds on \bar{X} and σ which maximize z . Choose the region

$$a < \bar{X}$$

which makes sense; a designer would never consider using a stress value above the average. To maximize z , we take the experimental statistics \bar{X}, s and find a one-sided 95% confidence lower bound for \bar{X} , and upper bound for s .

Using standard techniques for interval estimation [Hays and Winkler], a lower 95% confidence limit for the average is*:

$$\bar{X}_L = \bar{X} - \frac{t^*S}{\sqrt{n}} \quad (27)$$

where t^* = "t" statistic (1.708 for this case)

S = standard deviation

n = number of data (25 for this case)

The results of this calculation are in Table 5. Similarly, an upper 95% confidence limit for S may be found using the Chi-squared distribution (χ^2) as:

$$S_u = S \sqrt{\frac{(n-1)}{\chi^2_{(n-1;0.95)}}} \quad (28)$$

where n = number of data (25 here)

$\chi^2_{(n-1;0.95)}$ = Chi-squared for $n-1$ degrees of freedom, up to 95% (13.85 here)

These results are also shown in Table 5.

As an example of this conservatism, take material "A" under an applied stress of 19,000 psi. The results using the experimental statistics directly are:

$$z = \frac{19,000 - 22,500}{1720}$$

$$P[\sigma_s \leq 19,000] = \Phi(-2.03) = 2.1 \% \text{ probability of failure}$$

If we use bounded estimates of the experimental statistics,

* If μ is the true population mean, then

$$\text{Probability } [X_L \leq \mu < \infty] = 0.95$$

we get

$$z = \frac{19,000 - 21,900}{2270} = -1.28$$

Probability of failure 10.0%

That is, the use of conservative bounds on our estimates causes us to maximize our predicted probability of failure.

Table 5
Lower Bound Averages for Normal Statistics

Material	\bar{X} (psi)	S (psi)	X_L (psi)	S_u (psi)
A	22,500	1,720	21,900	2,270
B	25,400	2,080	24,700	2,750
C	83,600	4,220	82,200	5,570
D	165,000	4,780	163,000	6,310
E	112,000	4,100	111,000	5,410
F	19,300	968	19,000	1,280
G	31,600	395	31,500	520
I	32,300	949	32,000	1,250
J	55,600	3,920	54,300	5,170
L	72,900	7,270	70,400	9,590

3.4 Notch Sensitivity

The development which follows is primarily for materials which fail in a "net tension" mode when placed under tension with a notch perpendicular to the applied load. (See fig. 1.) This failure mode could also be referred to as "self-similar crack growth," since the notch growth is in the same direction as the original notch.

The details of this development may be found in [Pipes, Wetherhold and Gillespie]. Consider the variation of notch strength with notch length given by:

$$\frac{\sigma_N}{\sigma_0} = \left\{ 1 - (1 + C^{m-1} k^{-1})^{-2} \right\}^{1/2} \quad (29)$$

where

σ_N = notched tensile strength

σ_0 = unnotched tensile strength

C = notch half-length

k = notch sensitivity factor

m = exponential factor, $m < 1$

The use of equation (29) requires a minimum of two notch sizes to determine the empirical parameters m , k . Once these are found, equation (29) allows prediction of notch strength over a wide variety of notch sizes. The method used to calculate m and k was by minimizing

the squared error between the curve (29) and the data. Increasing m and k increases the notch sensitivity (faster strength reduction in the presence of a notch).

Table 6 shows the notch sensitivity factors for the materials tested. Material G was too narrow for notch testing; Material D showed extensive axial splitting and endtab debonding. The difference in the notched strength values caused by the finite width corrections (see Table 2) are not significant, and so either σ_N or σ_N^∞ could be used. Figures 16 through 23 show plots of the notched strength versus notch size.

Table 6
Notched Strength Parameters

Material	Crack length 2 c (inch)	σ_N/σ_0	Notch Sensitivity	
			Parameters m	k
A	0.126	0.97		
	0.250	0.74	-0.63	49.8
	0.375	0.66		
B	0.125	0.95		
	0.253	0.77	-0.62	46.6
	0.375	0.66		
C	0.127	0.79		
	0.250	0.69	0.11	18.1
	0.375	0.59		
D	AXIAL SPLITTING, ENDTAB DEBONDING see Section 4			
E	0.125	0.87		
	0.250	0.79	0.0	14.1
	0.375	0.68		
F	0.125	0.68		
	0.250	0.54	-0.03	47.4
	0.375	0.44		
G	NOT TESTED - too narrow			
I	0.125	0.82		
	0.256	0.69	-0.04	23.6
	0.375	0.58		
J	0.125	1.02		
	0.250	0.82	-0.69	50.0
	0.375	0.61		
L	0.125	0.94		
	0.250	0.73	-0.37	31.3
	0.375	0.67		

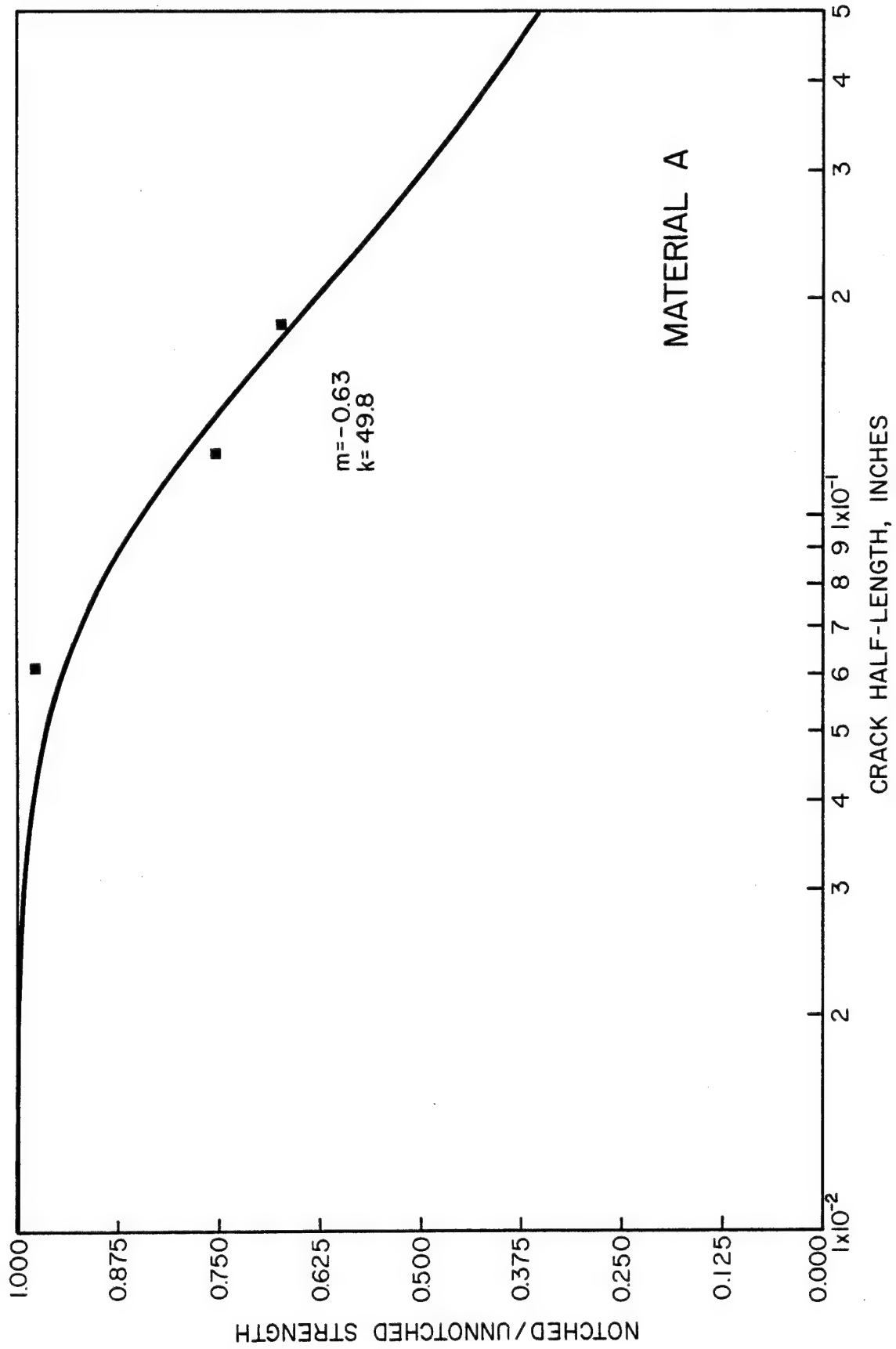


Figure 16.

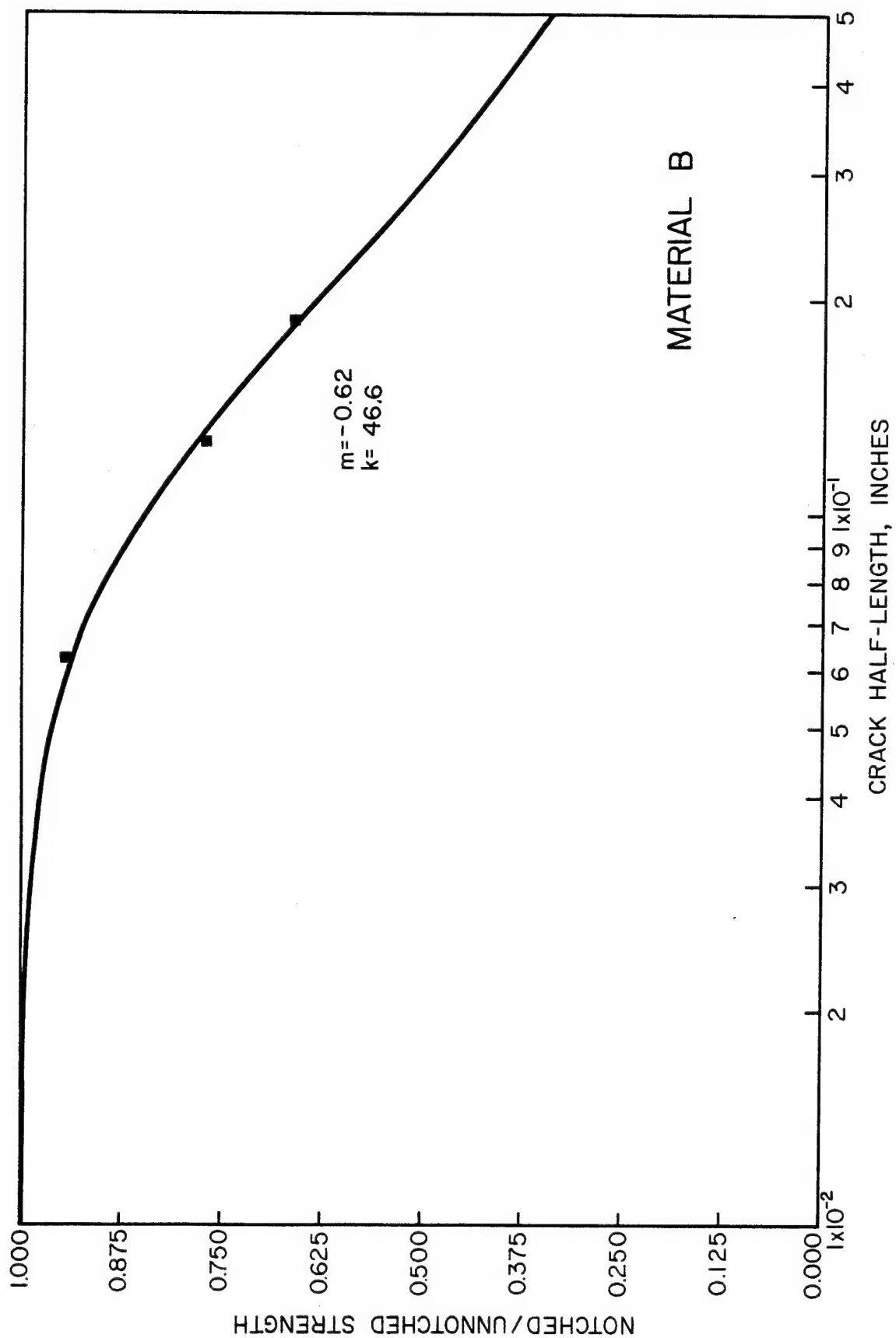


Figure 17.

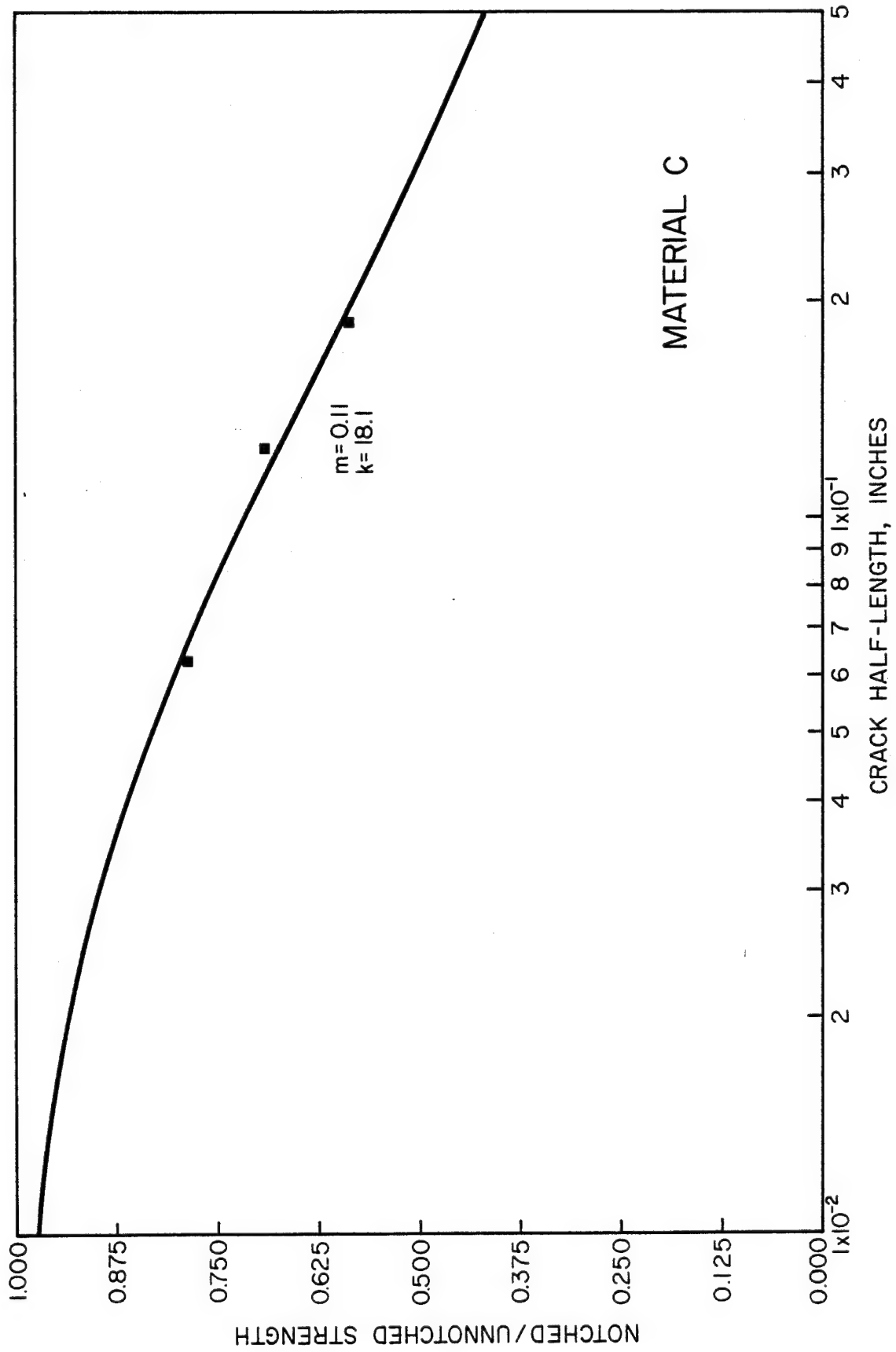


Figure 18.

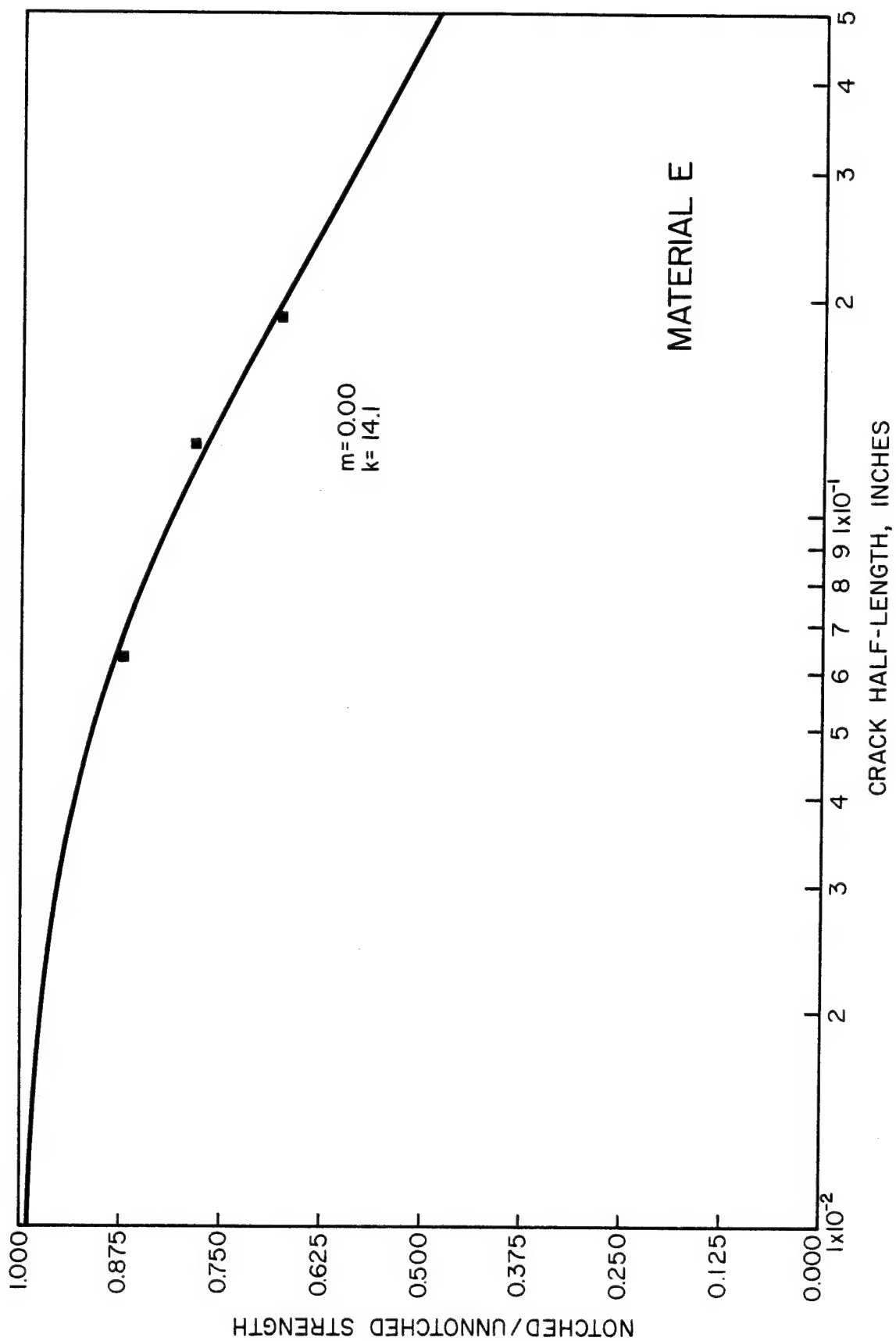


Figure 19.

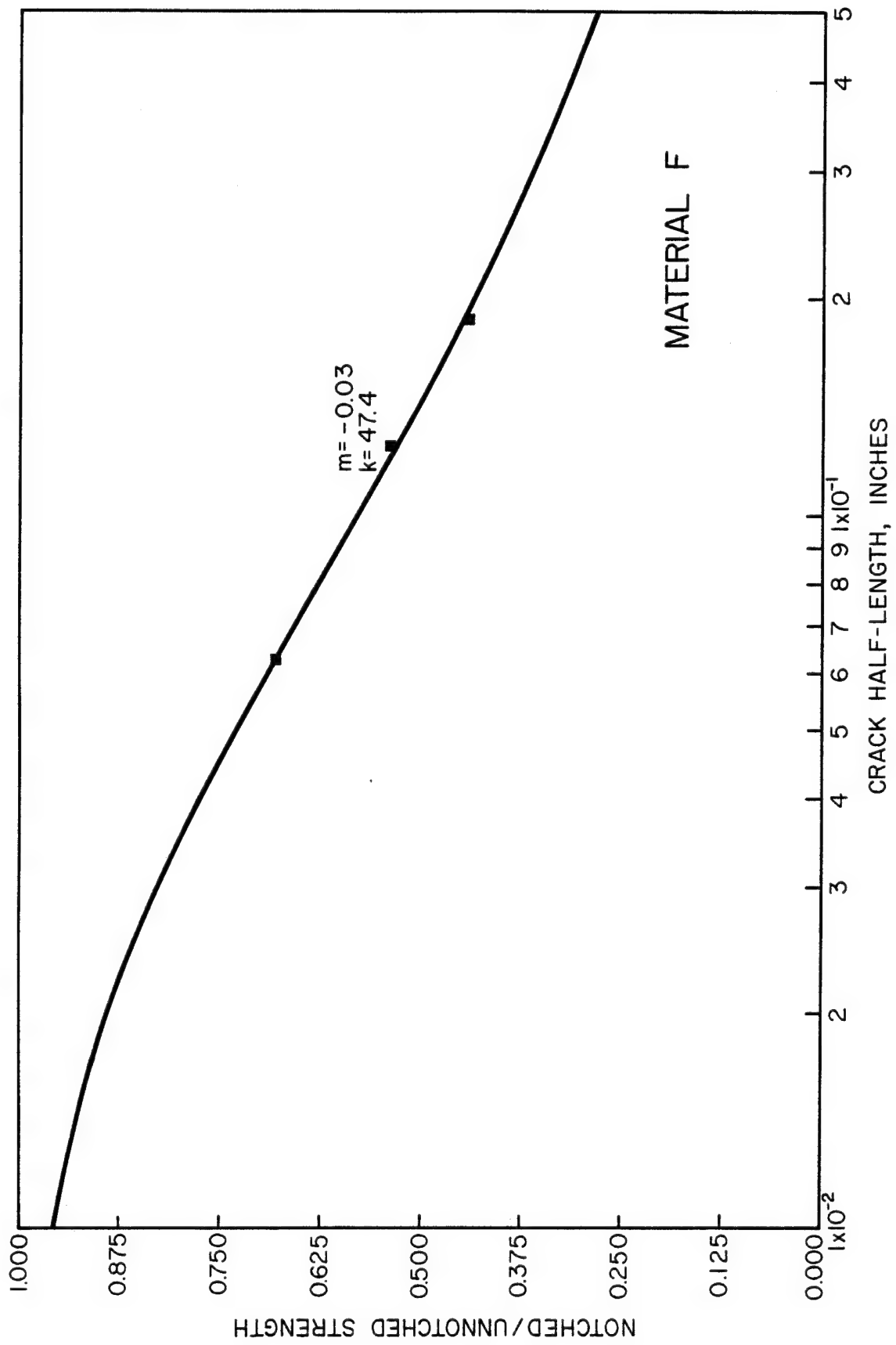


Figure 20.

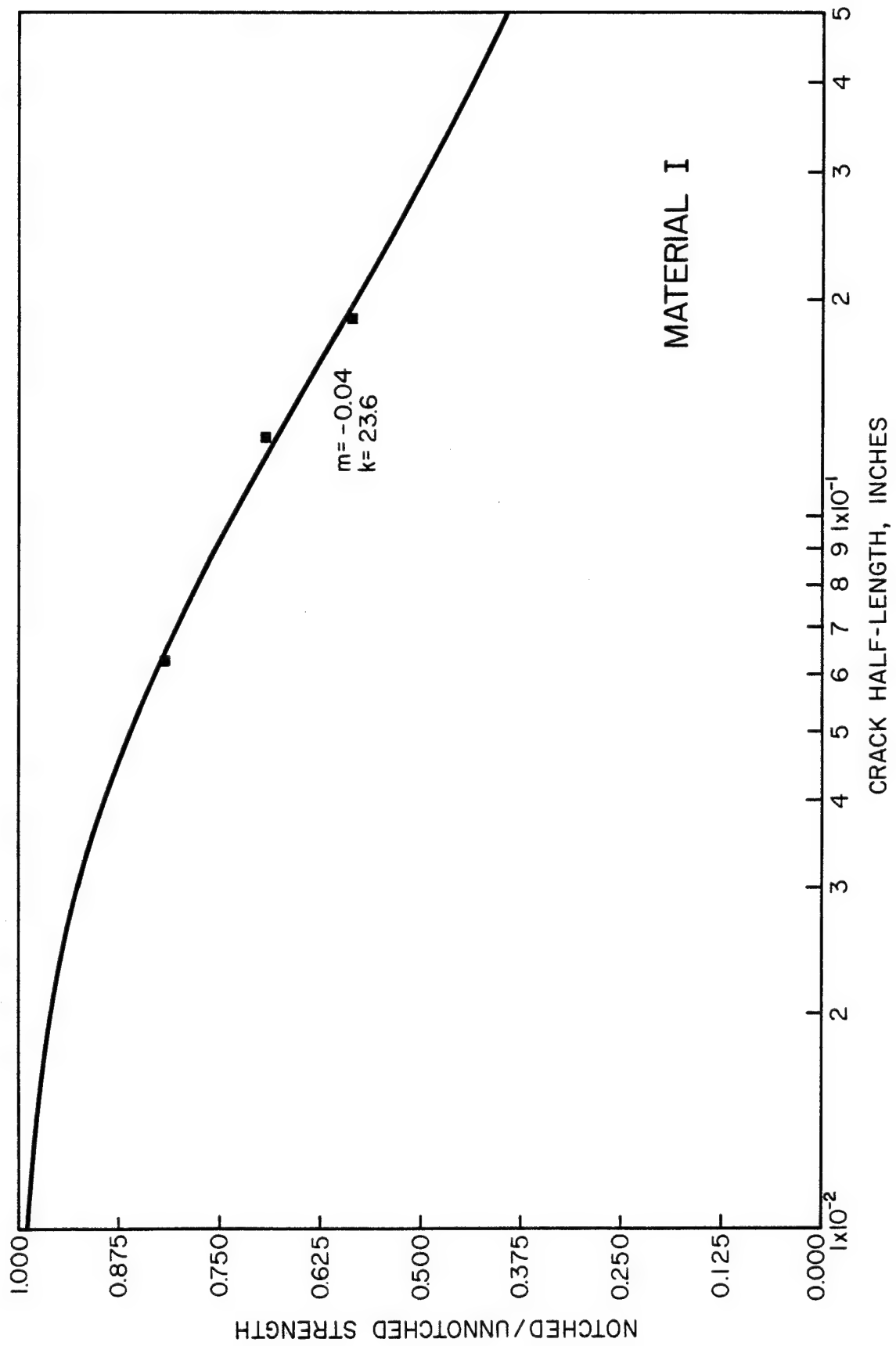


Figure 21.

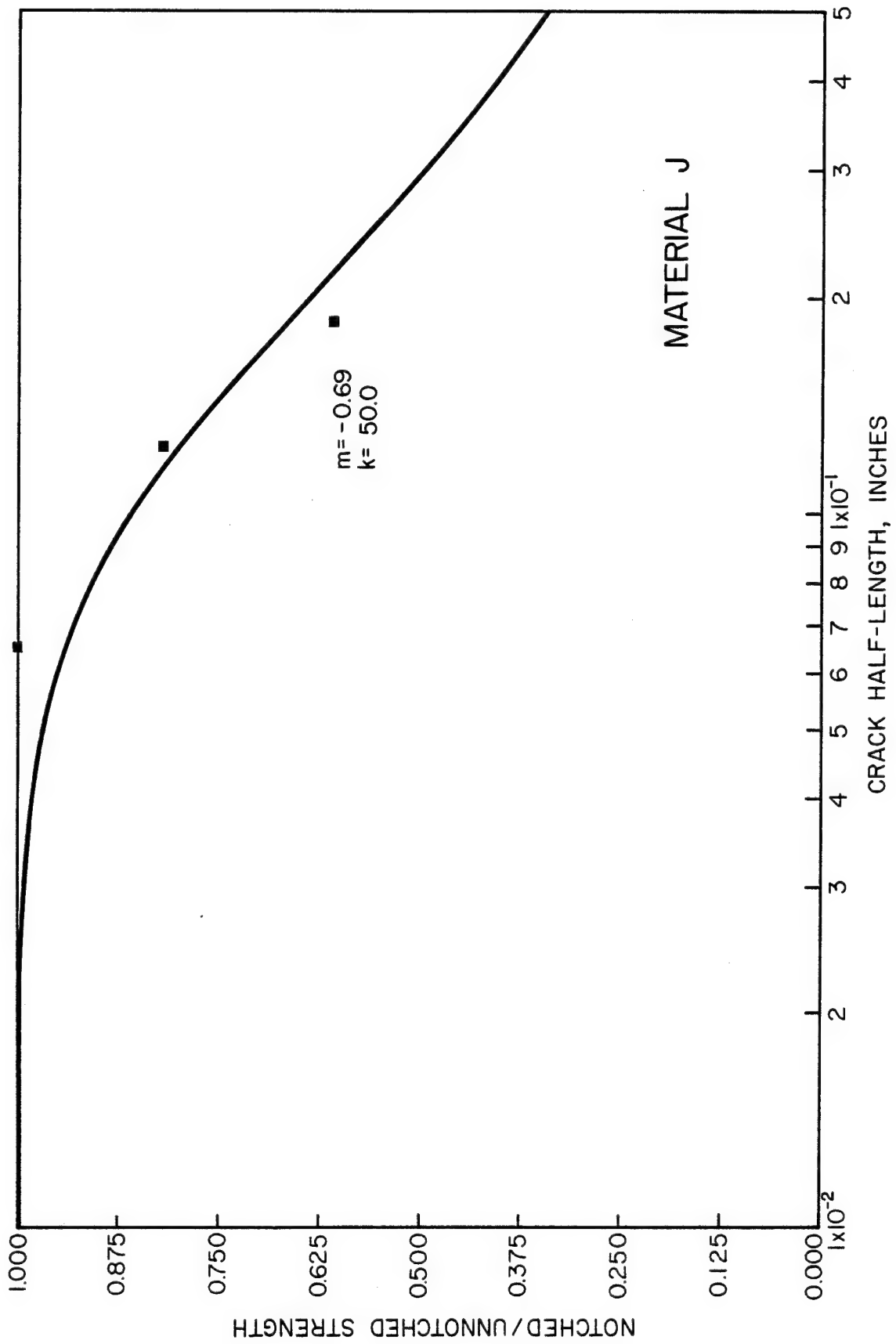


Figure 22.

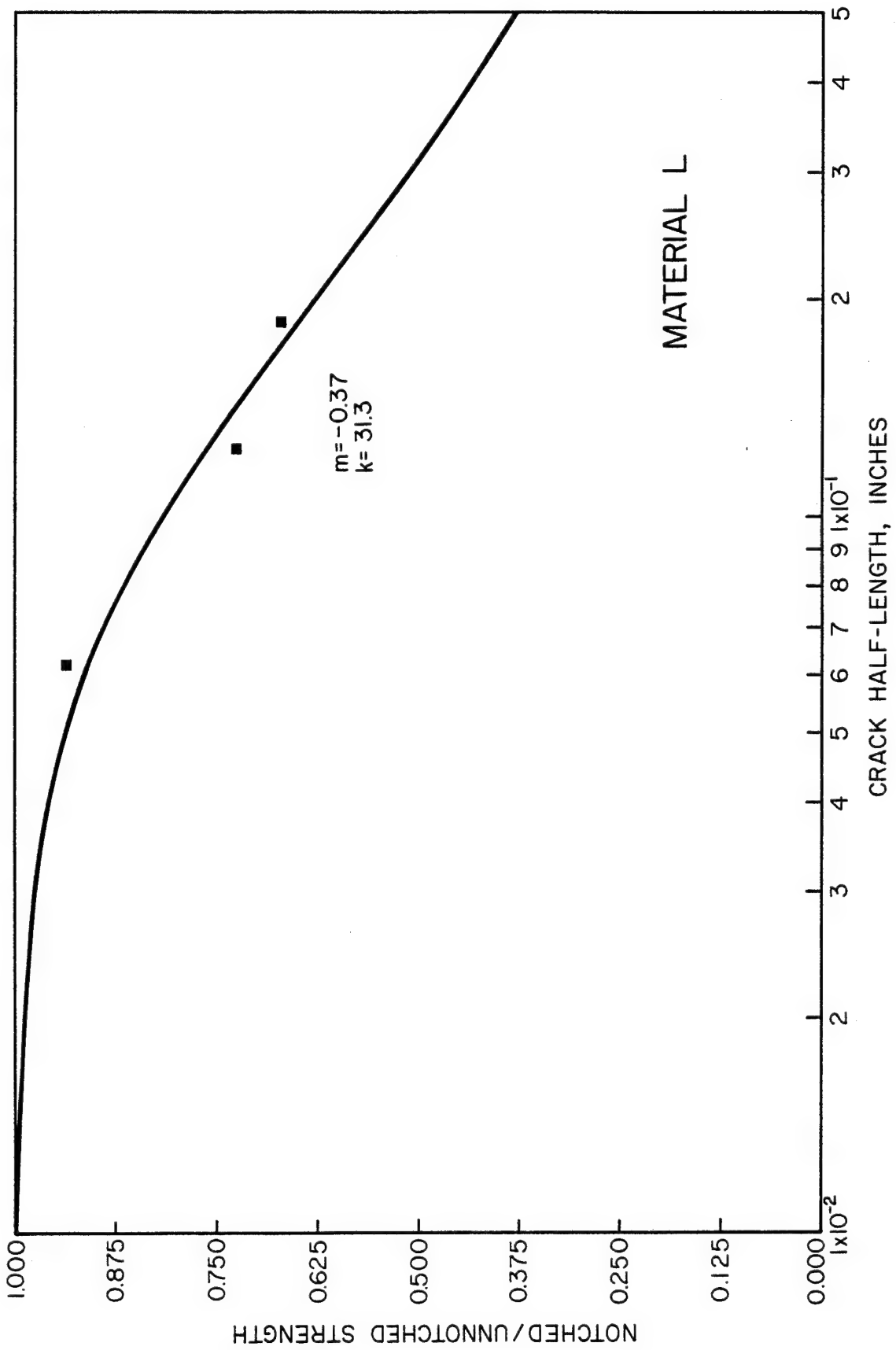


Figure 23.

4. Discussion and Conclusions

Data and Statistics

Data have been given for the tensile strength and its degree of variability for a variety of composite material systems. The data fit a Weibull distribution well, and conservative parameters are given which allow reliability predictions. The advantages of a Weibull distribution include:

- Reliability can be calculated in closed form, without using tables
- Results agree with intuition on "weak link" or brittle failure modes [Weibull].

The development for calculating Weibull, normal, and log normal statistics from data and developing conservative design parameters is given in detail. The results are uniformly conservative for all materials tested. (See Figures 6 through 15). The theoretical relation between tensile and flexural strengths is also given.

Data Variability

The degree of tensile data scatter for most of the materials tested was virtually identical. The average shape parameter α (reflects the data scatter) is:

- $\alpha = 29.5$ average for all materials tested
- $\alpha = 20.0$ average for press-molded materials

The press-molded materials have higher data scatter; to design to a given degree of reliability, we must utilize a smaller fraction of their average strength.

The two materials (D and G) exhibiting the smallest scatter were a pultruded and an injection molded material. These are continuous or automated processes in which one expects a higher degree of repeatability. The other injection molded material (F) probably loses its repeatability due to the machining process.

The hybrid materials might be expected to have minimal data scatter due to the presence of continuous graphite reinforcement. However, the degree of scatter is comparable to that of most SMC materials. There are two possible explanations for this. The chopped glass participates heavily in the fracture process, and often delaminates from the graphite face sheets. The inherent variability of a chopped glass compound thus comes into play. Secondly, the present process of producing the hybrid is as a laboratory batch process. As production methods are stabilized into a standard process, the variability should decrease.

Notched Strength

Data are presented for the notched static strength of the materials, and show a good fit to the model. The parameters required to predict notched strength over a wide range of notch sizes are given. Since the notch geometry is the most severe test, use of the strength formula for notches should give a conservative prediction is used for circular, slot, or elliptical holes.

The use of the model (equation 29) gives superior results to those of classical "critical stress intensity factor" approach. If this approach, used in linear elastic fracture mechanics (LEFM), were valid, the k_{IC} value in Table 2 would be a constant independent of hole size for a given material. It is emphatically not constant; k_{IC} increases with increasing notch size for every material tested. Models such as those in [Pipes, et al.] which account for the integrated effect of stress over a volume appear best suited to explain the hole size effect in composites.

Several materials tested showed little strength change for small notches. This gives an indication of the size of inherent flaws. That is, if placing a 1/8" notch does not affect strength, the inherent flaw distribution of an

unnotched sample must contain flaws on the order of 1/8". This could be used as a quality control mechanism, since a large inherent flaw size indicates a potentially low strength material.

Relationship between Notch Sensitivity and Tensile Data Variability

It has been proposed from theoretical grounds that the degree of tensile strength data scatter should be related to the notch sensitivity for a brittle material [Wetherhold]. The prediction is that a material with a high degree of data scatter should be relatively insensitive to the presence of a notch. Both properties rely on the size and distribution of inherent flaws. A high α value arises from a very narrow spread of tensile strength data. This implies that the size and distribution of inherent flaws are also very narrowly distributed. Due to the inherent "perfection" or repeatability of a high α material, the addition of a flaw or notch has a dramatic effect on the strength.

The results of this testing program suggest that this relationship is true, but the returns are fragmentary. The highest α material (G) was too narrow to test with notches. The pultruded material (G) showed low scatter

(high α) in flexure, but the notch sensitivity results are extremely incomplete due to axial splitting and "brooming" of fibers. Nonetheless, the results suggest an extremely rapid strength degradation in the presence of a small notch. See Table 7. These results are not presented in Table 2 due to their incomplete nature.

Table 7

Crack Length 2c (inch)	σ_N/σ_0	Number of Specimens
0.125	0.66	2
0.250	0.63	4
0.375	0.53	2

$\sigma_0 = 150,000$ psi (see Section 3.2)

Specimen dimensions were as shown in figure 1.

At the other end of the spectrum, examine the hybrid material J, which exhibits little strength degradation in the presence of a small (0.125") notch. This material also has a fairly large data scatter (low α), which is consistent with prediction. There are, however, enough ambivalent results that the conclusions must be considered tentative. (See material I, for example.)

References

- R. E. Bullock, "Strength Ratios of Composite Materials in Flexure and in Tension," J. Comp. Materials V. 8, April 1974, pp. 200-206.
- W. L. Hays, R. L. Winkler, Statistics Vol. 1, Holt, Rinehart & Winston, 1970, pp. 327-333, 357-359.
- N. R. Mann, R. E. Schafer, N. D. Singpurwalla, Methods for Statistical Analysis of Reliability and Life Data, John Wiley & Sons, New York, 1974.
- W. Mendenhall and R. Scheaffer, Mathematical Statistics with Applications, Duxbury Press, 1973.
- P. C. Paris, G. C. Sih, Fracture Toughness Testing and its Applications, ASTM STP 381, American Society for Testing and Materials, 1965, pp. 84-113.
- R. B. Pipes, R. C. Wetherhold, J. W. Gillespie, Jr., "Macroscopic Fracture of Fibrous Composites," Materials Science and Engineering, Vol. 45, No. 3, October 1980.
- D. R. Thoman, L. J. Bain, C. E. Antle, "Inferences on the Parameters of the Weibull Distribution," Technometrics, Vol. 11, No. 3, 1969.
- W. Weibull, "The Phenomenon of Rupture in Solids," Ingeniörs Vetenskaps Akademien Handlingar Nr. 153, Stockholm, 1939 (in English).
- R. C. Wetherhold, J. M. Whitney, "Tensile Failure of Notched Fiber-Reinforced Composite Materials," Polymer Composites, to be published.
- J. M. Whitney and M. Knight, "The Relationship Between Tensile Strength and Flexure Strength in Fiber-Reinforced Composites," Exp. Mechanics V. 20, June 1980, pp. 211-216.